DEVELOPMENT OF A COASTAL FUMIGATION MODEL FOR CONTINUOUS EMISSION FROM AN ELEVATED POINT SOURCE AND A COMPUTER SOFTWARE (FUMIG)

MUDDASSIR NAZIR

NOTE TO USERS

10

Development of a Coastal Fumigation Model for Continuous Emission from an Elevated Point Source and a Computer Software (Fumig)

by

© Muddassir Nazir

A thesis submitted to the

School of Graduate Studies

in partial fulfillment of the

requirements for the degree of

(Master of Engineering)

Faculty of Engineering & Applied Science
Memorial University of Newfoundland

May, 2004

St. John's Newfoundland

Your file Votre référence
ISBN: 0-494-02365-1
Our file Notre référence
ISBN: 0-494-02365-1

Abstract

A fumigation model based on probability density function (PDF) approach is presented here to study the dispersion of air pollutants emitted from a stack on the shoreline. This work considers dispersion of the pollutants in the stable layer and within thermal internal boundary layer (TIBL) proceeds independently. The growth of TIBL is considered parabolic with distance inland and turbulence is taken as homogeneous and stationary within the TIBL. Dispersion of particles (contaminant) in lateral and vertical directions is assumed independent of each other. This assumption allows us to consider the position of particles in both directions as independent random variables. The lateral dispersion distribution within the TIBL is considered as Gaussian and independent of height. A skewed bi-Gaussian vertical velocity PDF is used to account for the physics of dispersion due to different characteristics of updrafts and downdrafts within TIBL. Incorporating finite Lagrangian time scale for the vertical velocity component, it is observed that it reduces the vertical dispersion in the beginning and moves the point of maximum concentration further downwind. Due to little dispersion in the beginning, there is more plume to be dispersed causing higher concentrations at large distances. The model has considered Weil and Brower's (1984) convective limit to analyze dispersion characteristics within TIBL. The revised model discussed here is evaluated with the data available from the Nanticoke field experiment on fumigation conducted in the summer of 1978 in Ontario, Canada. The results of the revised model are in better agreement with the observed data, as compared to other available models. The study suggests the use of

mean absolute error and mean relative error as quantitative measures of model performance along with the residual analysis.

For easy and effective use of the newly developed model, user-friendly computer software 'Fumig' is developed in visual basic. Fumig is built upon the developed model and enable easy assessment of concentration profiles under fumigation conditions.

Keywords: Air pollution dispersion, coastal fumigation, thermal internal boundary layer, probability density function technique, finite vertical Lagrangian time scale.

Acknowledgements

I would like to extend my deep gratitude to my supervisor Dr. Faisal I Khan who guided me and supported me financially throughout the course of my Master of Engineering degree. Without his untiring and selfless cooperation I would have never been able to achieve the present level of understanding and the quality of my research work.

I am personally indebted to my co-supervisor Dr. Tahir Husain for his overwhelm encouragement and moral support throughout the course of my degree. He also gave me insight into the subject of Air Pollution Modeling and guided me through basic and higher concepts of the subject.

I express my thanks to Dr. Michael Booton, Dr. James Sharp and Dr. Leonard Lye for imparting me with valuable knowledge through teaching of various courses during my Master of Engineering degree.

In the end I thank my parents for their wholehearted support, encouragement and blessings. They have not only very kindly supported me morally during my hectic study hours but also borne partial expanses of my Master of Engineering degree at Memorial University of Newfoundland.

Table of Contents

List of Tables

List of Figures

List of Symbols[1]

[M]	mass
$\|N\|$	number of times reflection occurs from the TIBL top
[L]	length
[T]	time
A_o	TIBL height parameter
b	obtained from a laboratory study of the fumigation phenomenon, carried out by Hibberd and Luhar (1996)
B_o	bowen ratio
c_p	specific heat at constant pressure
$\hat{C}$	transformed concentration
$C(x,y,0)$	ground level air pollutant concentration by Models of Van Dop et al. (1979) and Misra (1980)
$C(x,y,z;H)$	air pollutant concentration by Gaussian plume model
$C(x,y,z<z_i(x))$	air pollutant concentration at any distance downwind within TIBL by new model
$C(x,y,z\le z_i:H)$	air pollutant concentration within TIBL by using the Lyons and Cole (1973) model
$C(x',y,z\le z_i:H)$	air pollutant concentration in the third (trapped zone) by using the Lyons and Cole (1973) model
$\hat{C}_o(x_1,x_2)$	observed concentration during experiment

[1] If the above illustration of any symbol conflicts with the illustration of that symbol given in the following literature then preference should be given to the illustration, provided in the following chapters.

$\hat{C}_p(x_1)$	predicted concentration by model
$C_s(x', y', z; H)$	concentration field within the stable layer
d	the number of the day of the year
d_r	the day of the summer solstice (173)
d_y	the average number of days per year (365.25)
$dC\left(x, y, z < z_i \middle\| x', y', z_i(x)'\right)$	concentration at any distance downwind within the TIBL associated with elemental source strength $dQ(x', y', z')$
$dQ(x', y', z')$	elemental source strength associated with the infinitesimal arc
D_s	inside diameter of the stack exit
f_{ly}	function that satisfies the short and long time limits in the lateral direction
f_{lz}	function that satisfies the short and long time limits in the vertical direction
$F(x', y', z')$	flux from the concentration field in the stable layer to the TIBL through an infinitesimal arc
F_o	buoyancy flux
g	acceleration due to gravity
H	effective height of the centerline of the pollutant plume
H_f	sensible heat flux
K_{zs}	diffusivity coefficient in the stable layer
n	cloud cover (0-1.0)

N	sample size
N_e	Brunt-Vaisala frequency
P_a	ambient air pressure
P_o	ground level pressure (in meteorology it is common to take 1000 mb)
$p_w[w(z)]$	probability density function for the random vertical velocity within convective layer
p_w^{Σ}	probability density function for the random vertical velocity within convective layer summed up over all w values to include reflections at the boundaries
$p_y\left(y;\frac{x}{U}\right)$	density of particle position in y at time t (where t is $\frac{x}{U}$)
$p_z\left(z;\frac{x}{U}\right)$	density of particle position in z at time t (where t is $\frac{x}{U}$)
$p_{yz}\left(y,z;\frac{x}{U}\right)$	joint density of particle position in y and z at time t (where t is $\frac{x}{U}$)
Q	pollutant emission rate
r	plume radius
$r\{\phi\}$	albedo
R	Weil (1990) parameter
R_n	net radiation
R_s	solar radiation
S	vertical velocity skewness

t_{UTC}	coordinated universal time in hours
T	averaging time period (usually taken as 1 hour)
T_a	ambient air temperature
T_{gs}	gas temperature at stack exit
T_{ly}	lateral Lagrangian integral time scale
T_{lz}	vertical Lagrangian integral time scale
T_{ref}	ambient Air Temperature at ground surface
T_s	surface temperature
u	instantaneous velocity component along the streamline (usually aligned with the x-axis)
u'	eddy or fluctuating velocity along the streamline
U	mean wind speed
U_s	mean wind speed in the stable layer
v	instantaneous velocity component along the y-axis
v'	eddy or fluctuating velocity along the y-axis
V	temporal average velocity component along the y-axis
w	instantaneous velocity component along the z-axis in Chapter 1 (elsewhere representing random vertical velocity in convective boundary layer)
w_j	random vertical velocity in updraft with j=1 and random vertical velocity in downdraft with j=2
w_*	convective velocity

w'	eddy or fluctuating velocity along the z-axis
$\overline{w}_j$	mean vertical velocity in updraft with j=1 and mean vertical velocity in downdraft with j=2
W	temporal average velocity component along the z-axis
x	distance co-ordinate in longitudinal direction
x_1	denotes model inputs
x_2	denotes unknown variables not included in the model
x_f	horizontal distance at which final plume rise is obtained
x_*	upper limit of the integral in Venkatram's (1988) model
x'	integration variable that corresponds to the location of an elemental source, at the plume-TIBL interface, between 0 and receptor location x, in the present model
y	distance co-ordinate in lateral direction
y'	integration variable that corresponds to the location of an elemental source, at the plume-TIBL interface, between $+\infty$ to $-\infty$ in the lateral direction, in the present model
z	distance co-ordinate in vertical direction
z_{eq}	TIBL equilibrium height
z'_{eq}	final plume rise
z_{fe}	height corresponding to the ending of the fumigation zone
z_{fs}	height which corresponds to the start of the fumigation zone
z_i	convective boundary layer height

z_{io}	height at which the plume centerline intercepts the TIBL
z_n'	transitional plume rise
z_s	source height
β	the ratio of the downward heat flux at the TIBL to the upward heat flux at the surface; its value is approximately 0.2 for the CBL over land
β_1	entrainment parameter (0.4-0.6)
γ	change of potential temperature with height
Γ	dry adiabatic lapse rate
$\varepsilon(x_2)$	residual which is due to unknown variables
δ	solar declination angle
ϕ	solar elevation angle
ϕ_r	latitude of the Tropic of Cancer (23.45^o=0.409 radians)
Ψ	latitude (positive north)
ρ	air density
λ	longitude (positive west)
λ_1	weighting coefficient for the updraft distribution
λ_2	weighting coefficient for the downdraft distribution
σ_{SB}	Stefan Boltzman constant
σ_v	root mean square lateral turbulence velocity
σ_w	overall root mean square vertical turbulence velocity within TIBL

σ_{wj}	standard deviation of vertical velocity in updraft with j=1 and in downdraft with j=2
$\sigma_y(x)$	standard deviation of the concentration distribution in the crosswind direction, at the down wind distance
$\sigma_y(x')$	standard deviation of the concentration distribution in the crosswind direction, at the down wind distance in the third zone of Lyons and Cole (1973) model
σ_{yf}	dispersion spread due to plume buoyancy in the lateral direction in the stable region
σ_{ys}	lateral dispersion coefficient in the stable layer used by Lyons and Cole (1973)
σ_{yfg}	horizontal spread of the plume in the fumigation zone in Lyons and Cole (1973) model
$\sigma_{yt}(x,x')$	lateral dispersion coefficient in TIBL used in the present model
σ_{yT}	lateral dispersion coefficient in TIBL used in Models of Van Dop et al. (1979) and Misra (1980)
$\sigma_z(x)$	standard deviation of the concentration distribution in the vertical direction, at the down wind distance
σ_{zf}	dispersion spread due to plume buoyancy in the vertical direction in the stable region
$\sigma_{zj}(x,x')$	root mean square vertical displacement in updraft with j=1 and in downdraft with j=2

σ_{zs}	vertical dispersion coefficient in the stable layer used by Lyons and Cole (1973)
$\sigma'^2(x')$	overall lateral dispersion coefficient within TIBL used in the present study
$\sigma'^2_M(x,x')$	overall lateral dispersion coefficient within TIBL used by Misra (1980)
$\sigma'^2_V(x,x')$	overall lateral dispersion coefficient within TIBL used by Van Dop et al. (1979)

Chapter 1

Introduction

1.1 The Air Pollution Problem of a Coastal Region and the Role of Environmental Engineer in Controlling the Problem:

Air pollution problem in the coastal region is of serious concern because of population growth and industrialization within the coastal region. A coastal fumigation phenomenon, which occurs due to the entrainment of plume into inland growing thermal internal boundary layer (TIBL), is responsible for high ground level concentrations.

There are many industrial disasters related to air quality in the coastal region. London Smog episode, which resulted in around 4,000 deaths in the city in 1952, is one illustrative example of such episodes.

Air is used as a medium for dispersion of pollutants emitting out of stacks, chimneys and other sources in an industrial region. These pollutants are found in the form of gases (e.g., sulfur dioxide SO_2) or in the form of particulate matter (e.g., fine dust). Their dispersion is greatly influenced by meteorological parameters like the prevailing winds and atmospheric stability. Dispersion of pollutants also depends on the stack height and its cross-sectional area. If no control is done of these pollutants then at some distance downwind they reach a level where they may have adverse effects on human health, environment and ecology. It is the duty of an environmental engineer to predict the atmospheric capabilities to transport and disperse a pollutant under different meteorological conditions, and to design the air quality management strategies

accordingly. The ultimate objective is to ensure the pollutant concentration levels remain within the permissible regulatory standards at any location downwind.

1.2 Fumigation:

The dispersion in the coastal region is effected by the growth of Internal Boundary Layer. The boundary layer is the region in which the atmosphere experiences surface effects through vertical exchanges of momentum, heat and moisture.

Airflow across coastline (henceforth referred to as onshore flow), results into a spatially growing internal boundary layer due to differences in the physical properties of the land and water surfaces such as surface roughness and temperature. A mechanically forced internal boundary layer develops as the result of an abrupt change in surface roughness. However, when an onshore flow encounters the shoreline during the day with clear skies, the mechanical internal boundary layer is generally dominated by the thermal effects of the ground that give rise to the development overland of a thermal internal boundary layer (TIBL).

For the Growth of TIBL onshore, the following conditions must be met:

- onshore wind (Sea breeze)
- land is warmer than sea
- air over sea is stably stratified

Under such conditions, the air above the TIBL, representing the (undisturbed) onshore flow, maintains a stable (or neutral) vertical potential temperature gradient, whereas the upward heat flux from the ground tends to produce convection, the extent of which defines the boundary-layer height (or depth).

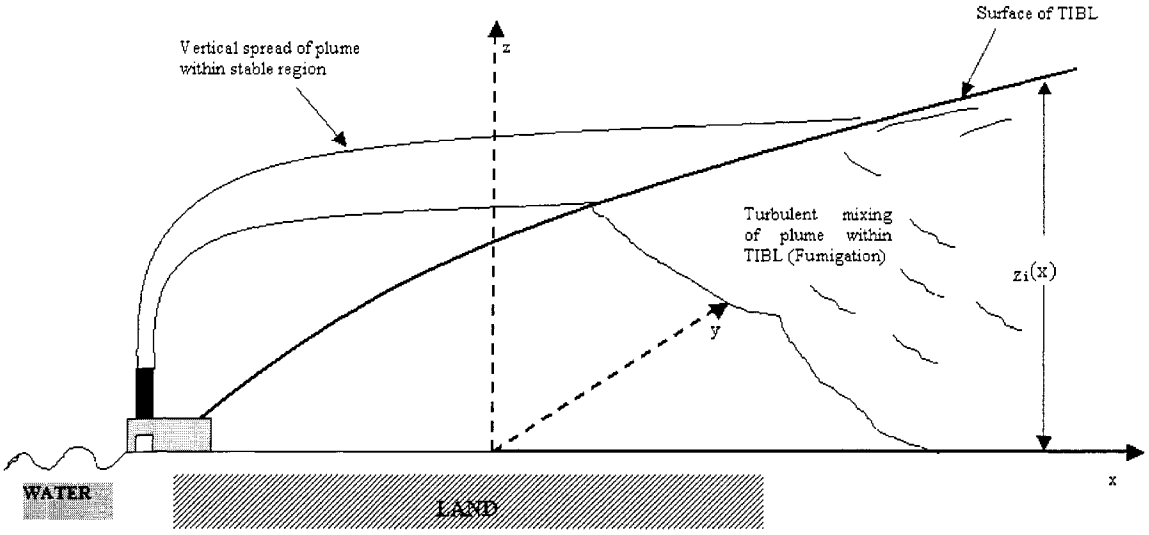

Figure 1.1 Typical dispersion pattern in coastal region

Coastal fumigation is a turbulent dispersion process in which a plume, from an elevated continuous point source, traveling in a stable onshore flow with relative little diffusion is intercepted by the growing TIBL. The plume is then subsequently mixed down to the ground by the large scale convective eddies and this may result in high ground level concentration of pollutants (c.f. Figure 1.1).

An environmental engineer should be able to predict the concentrations of the pollutants along the affected reach. Experimental methods are very expensive in this regard and cannot be employed in every coastal region. Therefore a predictive theory is required which can produce realistic concentration profiles with a minimum number of measurements. Also it is not possible to make measurements of resulting air quality for a facility that has not yet been constructed. So air dispersion modeling is the only way to estimate this future impact.

Mathematical models of fumigation have been developed to compute the concentration distribution using analytical techniques appropriate for routine and regulatory applications. In these models the Lagrangian time scale for random vertical velocity (w) is infinite so that the particle velocity at any downwind distance (x) is uniquely determined by its initial velocity. Mason's (1992) dispersion simulations using a Lagrangian model and large-eddy simulation fields show that a systematic reduction in vertical dispersion occurs with increasing wind speed. In the present work a revised analytical fumigation model by incorporating a finite Lagrangian timescale is developed for vertical dispersion, under sea breeze and strong convective conditions.

1.3 Some Basic Definitions and Concepts:

- **Turbulence:** Turbulence is essentially the motions of the wind over the time scales smaller than the averaging time used to determine the mean wind. Turbulence, the gustiness superimposed on the mean wind, can be visualized as consisting of irregular swirls of motion called eddies. Usually it consists of eddies of different sizes superimposed on each other.
- **Buoyant Generation of Turbulence:** The heating or cooling of air near the surface of earth causes buoyant turbulence. During sunny mid-day with light winds, solar heating of the ground causes large columns of buoyant air to rise. These large columns of rising buoyant air are referred as thermals. At night with light winds, the outgoing infrared radiation cools down the ground and the air adjacent to it. However, at some considerable height from the ground the temperature of the air remains relatively unchanged. This phenomenon results into a temperature inversion above the ground and downward heat flux from the air. Negative buoyancy stems from the influence of the inversion, which causes the atmosphere to stabilize and resist vertical motions. The negative buoyancy will even damp out some of the mechanical turbulence.
- **Mechanical Turbulence:** Frictional drag on the air flowing over the land causes wind shears to develop, resulting into mechanical turbulence. Obstacles like buildings deflect the airflow and cause turbulent wakes (adjacent to, and downwind of the obstacle).

- **Mean and Eddy Velocities:** If the flow is turbulent, the instantaneous velocity component (u) along the streamline will fluctuate with time even if the flow is steady. The average value of u over the period of time (T), usually taken as 1 hour, determines the temporal mean value of velocity (U) at a fixed point. This is illustrated in Figure 1.2 and U is evaluated for any finite time T as:

$$U = \frac{1}{T}\left(\int_{t_o-\frac{T}{2}}^{t_o+\frac{T}{2}} u\,dt\right) \tag{1.1}$$

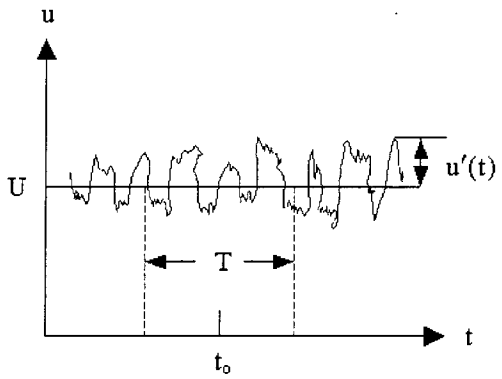

Figure 1.2 Definition of mean and eddy velocities

The difference between u and U at any instant, which is designated in Figure 1 as u', is called the eddy or fluctuating velocity. This fluctuation due to turbulence of the flow may be either positive or negative. Thus at any instant

$$u' = u - U \tag{1.2}$$

If the mean wind (streamline) direction is aligned with the horizontal x-axis and there is no significant large vertical motion then the average velocity components V and W in lateral (y) and vertical (z) directions respectively are negligible. Thus at any instant for eddy velocity components along y and z directions are $v' = v$ and $w' = w$, respectively.

The temporal mean values of eddy velocity components are zero

$$\overline{u'} = 0 ; \overline{v'} = 0 ; \overline{w'} = 0 \tag{1.3}$$

This implies that the time period is long enough within which positive and negative fluctuations associated with these components become equal.

Moreover the average of the square of eddy velocity is the statistical measure of the dispersion about the mean velocity, known as variance.

$$\sigma_u^2 = \overline{u'^2} ; \sigma_v^2 = \overline{v'^2} ; \sigma_w^2 = \overline{w'^2} \tag{1.4}$$

The square root of the variance is called standard deviation.

- **Ensemble Average:** The average value of the quantity taken over the identical experiments. For example, the ensemble average of the concentration c(x,t) is measured at point x at time t after many repeated identical trials. For turbulence that is both stationary and homogeneous (statistically not changing over time and space), the temporal and ensemble averages are equal. This is called the ergodic condition.
- **Advection:** Transport by an imposed current system, as the transport of pollutants in the atmosphere by wind.
- **Conduction**: Transfer of heat from molecule to molecule within a substance.
- **Convection:** Vertical transport induced by hydrostatic instability, such as the flow over a heated plate.
- **Free Convection:** If the fluid is initially at rest and no forces are present that would subsequently induce large-scale horizontal motion then small perturbations can initiate the transformation of the fluid's potential energy into kinetic energy.

Such motions are called free convection. Generally speaking, when buoyant convective process dominates, the atmosphere is said to be in a state of free convection.

- **Forced Convection:** In the situation where the fluid is driven horizontally by some external force, the motions are called forced convection. In atmosphere when mechanical process dominates, the atmosphere is said to be in a state of forced convection.
- **Sensible and Latent Portions of Heat Flux:** Transfer of heat per unit area per unit time is known as heat flux. Sensible heat flux removes heat from the ground surface to air due to the processes of conduction and convection. Conduction warms the very thin layer of air closest to the surface and convection transports this heat away from the surface to the surrounding atmosphere. In a latent portion of heat flux, the moist surface gets cooled (i.e. loses energy) through evaporation of liquid water at the surface of the earth. On the other hand, air gets warmed (i.e. gains energy) through condensation of water vapor in the atmosphere. Together this transport of latent heat acts to take energy away from the surface and transfer it to the atmosphere. Both of these fluxes reach a peak during mid-day at roughly the same time as the solar forcing peaks, and are small in the morning and evening. This supports the concept of partitioning the heat flux.
- **Bowen Ratio:** The Bowen Ratio is defined as the ratio of sensible to latent heat fluxes at the surface.

- **Albedo:** It is the ratio of the flux of solar radiation diffused by a surface to the flux incident upon it.
- **Potential Temperature:** It is the hypothetical temperature that would be achieved if air at an actual (ambient) temperature (T_a) and pressure (P_a) is compressed in an isentropic fashion to the ground level pressure P_o=1000 mb. It removes the temperature variation caused by changes in pressure altitude of an air parcel and is given by:

$$\theta = T_a\left(\frac{P_o}{P_a}\right)^{R/c_p} \tag{1.5}$$

Here R represents the specific gas constant for air and thermodynamic coefficient c_p is the specific heat at constant pressure.

The change of potential temperature with height (γ) is related to the change of temperature with height by:

$$\gamma = \frac{d\theta}{dz} = \frac{dT_a}{dz} + \Gamma \tag{1.6}$$

Where Γ is the dry adiabatic lapse rate and equal to 0.0098 K/m. The parameter γ is used to characterize the stability of the atmosphere. It will be positive for stable atmosphere; near to zero for neutral atmosphere; and negative for unstable atmosphere.

1.4 Characteristics of TIBL:

The characteristics of TIBL are similar to that of a mixed layer (ML) within a convective boundary layer. The mean characteristics of mixed layer are summarized as follows.

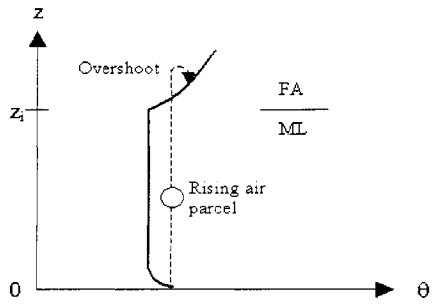

Figure 1.3 Overshooting of a rising air parcel

During the overshoot into the inversion, curtains of warm free atmosphere air are pushed into the TIBL and rapidly mixed down because of strong turbulence. This results into the entrainment of free atmosphere air into the TIBL. Thus the TIBL erodes into the free atmosphere.

The rate at which the air entrained into the top of TIBL is given by the entrainment velocity (w_e). The expression for entrainment velocity is discussed in chapter 4 and derived in Appendix 1.

1.5 Objectives of the Current Study:

The objectives of the current study are fourfold:

1. To develop a model, which can predict concentration distribution more reliably and efficiently under coastal fumigation conditions.
2. To undertake the sensitivity analysis of the model. This analysis will reveal sensitive input parameters to the model.
3. To evaluate and to validate the model performance by comparing the results with field data and already existing fumigation models.
4. To develop a computer code, based on the model, for easy (routine and regulatory) applications of the model.

1.6 Significance of Study:

Air quality models improve the effectiveness of air quality management. Through models, the contribution that exceeds the limit values from various sources is established. Based on the model estimates, air quality monitoring networks are designed. To monitor air quality for a facility that has not yet been constructed, air quality dispersion modeling is not just attractive but necessary.

Researchers have been trying to improve existing models to account for the coastal fumigation phenomenon, hydrodynamics of breeze effect and the consequent dispersion for the last three decades. Regulatory agencies such as US environmental protection agency (US EPA), has designed regulatory software packages based on these models by taking the advantage of high-speed computers. Two models, CALPUFF and AERMOD are among the latest US EPA regulatory models. CALPUFF deals with the coastal dispersion but AERMOD does not. However, CALPUFF model requires extensive set of meteorological data, which restricts its applicability to limited regions as discussed by Fisher et al (2003).

The significance of the study is to develop a fumigation model, which can account for the physics of the TIBL and its spatial growth. This model will be used in air quality modeling in coastal region. The model will be able to give more reliable concentration predictions and can be used in regulatory and monitoring purposes effectively in coastal region using routinely observed meteorological parameters.

1.7 Outline Of Thesis:

The literature review is presented in Chapter 2. This Chapter describes the available analytical models for coastal fumigation developed so far.

Chapter 3 encompasses the development of an analytical model for an elevated point source within the convective boundary layer. This model is then extended for the coastal fumigation case in Chapter 4. The parameters of this model are also explained in this Chapter.

Performance evaluation of the model with field study and its comparison with other fumigation models are done in Chapter 5. A sensitivity analysis of the fumigation model is undertaken in Chapter 6.

Chapter 7 presents the tool, based on the fumigation model, for easy applications. The concluding remarks and recommendations are given in Chapter 8.

Chapter 2

Literature Review

2.1 Introduction:

A number of studies have been conducted in the past to investigate the complex nature of dispersion process of air pollutants in the coastal environment. Various mathematical air pollution models have been developed to study the dispersion mechanism by considering the unique meteorological conditions present in the coastal region. These models are solved either analytically or numerically with the advent of high-speed computers.

This chapter provides a review of the studies related to air pollutant dispersion within the coastal region.

2.2 Coastal Dispersion:

Dispersion phenomenon in coastal region is unique because of the hydrodynamics of the breeze effect and consequent formation of TIBL with its height variation along the distance inland. Within the TIBL air is very unstable and turbulent. Above the TIBL the air is stably stratified and having the same characteristics as that of the over water air. The plume emitting from a stack located on a shoreline travels in the stable layer aloft with little diffusion unless it is intercepted by the TIBL. Within TIBL plume mixes rigorously because of turbulence and results into high ground level concentrations. This phenomenon is known as fumigation. Already existing fumigation models and their shortcomings are discussed in this section.

2.2.1 Gaussian Plume Model:

The Gaussian plume model is the most common air pollution dispersion model. This is based on mass balance approach and describes the three-dimensional concentration field generated by a point source under stationary meteorological and emission conditions. This model can be used in any situation where the distributions of velocities in both the horizontal and vertical directions are expected to be well represented by a Gaussian or normal distribution over the selected averaging time (usually an hour).

The model is expressed by:

$$C(x,y,z;H) = \frac{Q}{2\pi U \sigma_y \sigma_z} \exp\left[-\frac{y^2}{2\sigma_y^2}\right]\left[\exp\left[-\frac{(H-z)^2}{2\sigma_z^2}\right] + \exp\left[-\frac{(H+z)^2}{2\sigma_z^2}\right]\right] \qquad (2.1)$$

The variables used are:

C(x,y,z;H) Air pollutant concentration $\left[\frac{M}{L^3}\right]$

Q Pollutant emission rate $\left[\frac{M}{T}\right]$

U Wind speed at the point of release $\left[\frac{L}{T}\right]$

σ_y (x) The standard deviation of the concentration distribution in the crosswind direction, at the down wind distance [L]

σ_z (x) The standard deviation of the concentration distribution in the vertical direction, at the down wind distance [L]

H The effective height of the centerline of the pollutant plume [L]

Concentrations at the receptor downwind, calculated from the model, are directly proportional to the emissions and inversely proportional to wind speed. The greater the downwind distance from the source, the greater the horizontal spreading, σ_y, and the lower the concentration. The exponential term including the ratio of y to σ_y corrects for how far the receptor is off the center of the distribution in terms of standard deviations. Similarly, the greater the downwind distance from the source, the greater the vertical spreading, σ_z, and the lower the concentration. The sum of the two exponential terms account for the receptor height from the plume centerline before and after reflection. The term "H-z" represents the direct distance of the receptor from the plume centerline. The term "H+z" shows the reflected distance of the receptor from the plume centerline, which is the distance from the plume centerline to the ground (H) plus the distance back up to the receptor (z) after the reflection. Both σ_y and σ_z depend on downward distance (x) and are governed by atmospheric stability. This atmospheric stability depends on mechanical and buoyant turbulence. The most popular method for estimating atmospheric stability is based on the stability classification system proposed by Pasquill and then modified by Gifford. It is commonly known as Pasquill-Gifford (PG) system. To classify the atmospheric stability, the mechanical turbulence is considered by the inclusion of the surface wind speed (~ 10-meter above ground), in the PG system. The source of buoyant production of turbulence is the surface heat flux during daytime, which is driven by incoming solar radiation. The negative buoyant turbulence generation is considered

through the nighttime cloud cover. At night, the cloudiness is an indirect measure of the incoming thermal radiation, which counteracts the radiative cooling of the ground.

The PG system categories, which range from A (strongly unstable) to F (moderately stable), are each associated with curves for the dispersion measures σ_y and σ_z.

2.2.2 The Limitation of the Gaussian Plume Model Within CBL:

CBL consists of downdrafts and updrafts. Updrafts occupy ~ 40% of the horizontal area within CBL, the remaining ~ 60% area consists of downdrafts. Upward vertical velocities are higher in the updrafts than downward vertical velocities in the downdrafts (Lamb, 1982; Wyngaard,1988; Weil, 1988). This results in a non-Gaussian vertical velocity distribution. Samples of vertical velocity (Caughey, et al., 1983; Deardorff and Willis, 1985) measured both in updrafts and downdrafts typically show a positively skewed distribution with negative mode in the bulk of the CBL.

The plume centerline generally does not stay at the same height under convective conditions. For elevated sources the centerline descends until it reaches the ground and in contrast for ground level releases the plume lifts off the ground. This was verified by laboratory studies (Deardorff and Willis, 1975) and numerical simulations (Lamb, 1982).

For elevated sources, the centerline descent is explained by the greater areal coverage of downdrafts, and hence the higher probability of material being released into them. In addition, the downdrafts are long-lived so that material emitted into them tends to reach the surface.

For a surface source, material emitted into the base of an updraft begins rising almost immediately, whereas that released into downdrafts remains near the ground and moves horizontally. Since downdrafts occupy most of the horizontal area, more plume remains near the ground initially. However, after a significant amount of material is swept out of downdrafts and into neighboring updrafts, the plume centerline begins to lift off the ground.

Gaussian plume model predicts that an elevated plume centerline remains elevated until a sufficient number of particle reflections occur at the surface; the centerline then moves to surface, so do the maximum concentration.

It is concluded that a simple Gaussian model does not account for the dispersion characteristics of thermal internal boundary layer (TIBL), which forms on land during sea breeze conditions in coastal region, due to its convective nature.

2.2.3 The Lyons and Cole (1973) model:

Lyons and Cole (1973) modified Turner's nocturnal inversion breakup fumigation scheme for shoreline fumigation application. They used the model in a study of a fossil fuel plant located on the western shore of Lake Michigan. They considered a tall stack situated near the coast to describe the pollutant dispersion. The parabolic growth of TIBL over land was assumed during sea breeze conditions.

The Lyons and Cole model divides the downwind dispersion area into three zones and three different equations are used to determine the concentrations in those regions.

In the first zone the elevated plume is emitted into a homogeneous stable layer. The concentration is calculated with a simple Gaussian model within this zone. Plume dispersion in lateral and vertical direction is based on the PG criteria.

The second zone applies to the region where the plume impacts and is being entrained into the TIBL. The beginning of fumigation occurs at the point X_B on the TIBL interface where TIBL height is:

$$z_i=H-2.15\,\sigma_z \tag{2.2}$$

This is the position where the turbulence is just beginning to disturb the lower portion of the plume. Consequently, the point X_E at which the majority of the plume has been mixed into the TIBL is given by:

$$z_i=H+2.15\,\sigma_z \tag{2.3}$$

Within this region the lateral dispersion of plume is considered as Guassian while the vertical profile of concentrations below the TIBL is considered uniform. So the concentrations for $z \le z_i$, within this zone, are found by:

$$C(x,y,z \le z_i : H) = \frac{Q}{\sqrt{2\pi}\sigma_{yf} Uz_i}\left[\int_{-\infty}^{p}(2\pi)^{-\frac{1}{2}}\exp\left(-\frac{p^2}{2}\right)dp\right]\times\exp\left[-\frac{1}{2}\left(\frac{y}{\sigma_{yf}}\right)^2\right] \tag{2.4}$$

Where

$$p=\frac{(z_i-H)}{\sigma_{zs}} \tag{2.5}$$

$$\sigma_{yfg} = \sigma_{ys} + \frac{H}{8} \tag{2.6}$$

σ_{ys} and σ_{zs} are lateral and vertical dispersion coefficients in the stable layer, respectively.

σ_{yfg} is the horizontal spread of the plume in the fumigation zone. A correction factor of H/8 is thus added to σ_{ys} to account for increased dispersion in the TIBL.

The integral in Equation (2.4) is the area under the standard normal distribution and p is the value of a variable having the standard normal distribution. This gives the proportion of the normally distributed plume that has entered the TIBL at some distance X. Maximum ground level concentrations are predicted at distance X_E, where it is assumed that the entire plume has been mixed downward.

In the third zone the plume is assumed to be trapped with a variable lid (TIBL) height. Concentrations are assumed to be uniform in the vertical below the TIBL. Concentrations are estimated from $\sigma_y(x')$, a standard deviation based on x', the distance downwind from a virtual point source that lies between X_B and X_E. This way the overestimation of the lateral dispersion, which could be resulted by considering the actual distance from the source, is averted. The plume trapping formula is given as;

$$C(x', y, z \le z_i : H) = \frac{Q}{\sqrt{2\pi}\sigma_y(x')Uz_i} \times \exp\left[-\frac{1}{2}\left(\frac{y}{\sigma_y(x')}\right)^2\right] \tag{2.7}$$

2.2.4 Models of Van Dop et al. (1979) and Misra (1980):

Van Dop et al. (1979) derived a fumigation model by solving the advection-diffusion equation in the TIBL. In their model the fumigation of the plume, unlike the Lyons and Cole (1973) model, is not restricted to the fumigation zone but occurs everywhere at the interface between the stable and the mixed layer. Although this does not result in large changes of maximum surface concentrations but Van Dop et al. (1979) model leads to one consistent formulation of surface concentrations. The lateral concentration distribution in the mixed layer at a downwind distance x is considered to be originated from particles which have traveled in the stable and the mixed layer successively. This is reflected in the composite lateral dispersion coefficient, which contains the lateral dispersion coefficient of both layers.

Using a slightly different approach, Misra (1980) ends up with the same model as that of Van Dop et al. (1979). But he gives the different recipe for the lateral dispersion coefficient within the TIBL. Misra (1980) treats the net flux of material at each point (x, y) on the top of the TIBL as the source strength. The expression for ground level concentration within the TIBL is:

$$C(x,y,0) = \frac{Q}{\sqrt{2\pi}Uz_i(x)}\left[\int_0^x \frac{1}{\sigma'} \times \exp\left(-\frac{s^2}{2}\right)\frac{ds}{dx'}\right]\exp\left[-\frac{1}{2}\left(\frac{y}{\sigma'}\right)^2\right]dx' \qquad (2.8)$$

Where

$$s = \frac{[z_i(x') - H]}{\sigma_{zs}} \qquad (2.9)$$

$$\sigma'^2(x,x') = \sigma_{ys}^2(x') + \sigma_{yT}^2(x,x') \tag{2.10}$$

The terms σ_{ys} and σ_{zs} represent the dispersion coefficients in lateral and vertical directions, respectively, in the stable layer. Whereas σ_{yT} is the lateral dispersion coefficient in TIBL.

Misra assumes that the dispersion in the stable layer and in the TIBL are independent so that

$$\sigma_{yT}^2(x,x') = \sigma_{yT}^2(x-x') \tag{2.11}$$

Hence

$$\sigma'^2(x,x') = \sigma_{ys}^2(x') + \sigma_{yT}^2(x-x') \tag{2.12}$$

On the other hand, Van Dop et al. (1979) assumes:

$$\sigma_{yT}^2(x,x') = \sigma_{yT}^2(x) - \sigma_{yT}^2(x') \tag{2.13}$$

This implies that plume spread in the TIBL corresponds to particle release at the stack location assuming unstable conditions in the over water atmosphere.

Thus,

$$\sigma'^2(x,x') = \sigma_{ys}^2(x') + \sigma_{yT}^2(x) - \sigma_{yT}^2(x') \tag{2.14}$$

However, the assumption of unstable conditions in the over water atmosphere for calculating the plume spread in the TIBL is not justified.

2.2.5 The Deardorff and Willis (1982) Semi Empirical Model:

Deardorff and Wilis (1982) developed a model based on results from their water tank data. The model involves non-instantaneous mixing and accounts for the vertical variability in the TIBL height. The model variables are parameterized using the tank data. Its application is limited to fumigation conditions similar to those in the laboratory tank as mentioned by Luhar et al. (1996). DiCristofaro and Hanna (1990) also noted that the tank experiments were carried out at smaller entrainment rates than the equivalent TIBL slopes, which usually occur in coastal areas.

2.2.6 The Venkatram (1988) Model:

Venkatram's (1988) model is an extension of Misra's (1980) model. To account for the non instantaneous vertical mixing, he changed the upper limit of the integral in Equation (2.8) to x_* defined as:

$$x_* = x - 4z_i(x)U/w_* \tag{2.15}$$

Here $4z_i(x)/w_*$ is the time taken by the material to mix through the depth of the boundary layer. This is double the magnitude of the mixing time measured by Deardorff and Willis (1982) during their laboratory experiment. Testing of this modification, which assumes uniform vertical concentrations, has not been reported.

2.2.7 Lagrangian stochastic dispersion Models:

All the above stated fumigation models are Gaussian based and assume the instantaneous perfect vertical mixing of entraining plume. No provision is made in these models to account for the in-homogeneity and skewness of the vertical convective turbulence. This can lead to inaccurate predictions of concentration magnitude and location. Particularly when the growth rate of a spatially varying mixed layer is high and the vertical plume spread at the plume-TIBL interface is small.

Luhar and Britter (1990) used a one-dimensional stochastic dispersion model to overcome the above stated deficiencies in estimating the coastal fumigation concentrations.

Later, Luhar and Sawford (1995) extended the one-dimensional model to a two-dimensional stochastic model by incorporating the diffusion and gradients of flow properties in both the vertical and horizontal directions within the TIBL. The outcomes of this model show that the omission of diffusion and the gradients of flow properties in the stream wise direction do not influence the dispersion significantly. Normalized concentrations obtained from their model showed fair to good agreement with the results from Nanticoke field experiment and laboratory experiments of Deardorrf and Willis (1982). The major problem associated with this approach is that it requires large computational time and, therefore, is often not appropriate for operational and routine calculation.

2.2.8 Probability density function (PDF) Models:

The non-Gaussian vertical disprersion patterns of passive plumes during convective conditions were first discovered in the laboratory experiments by Willis and Deardorff (1976, 1978) and in numerical simulations by Lamb (1978, 1979). This non-Gaussian and asymmetric vertical diffusion is resulted from the differences between the vertical velocity distribution and strength of updrafts and downdrafts present during convective atmospheric conditions, as they relate to the ensemble-mean concentration distribution. Lamb (1982) calculated the probability density function (PDF) of the vertical velocity (p_w) from Deardorff's (1974) velocity field, which was computed by large eddy simulation. This analysis shows that turbulent energy in updrafts is higher than in down drafts and the mean velocity of updrafts is larger than those of down drafts. The PDF's of w at different boundary layer heights are positively skewed. The most probable velocity for each PDF is negative and approximately equal to the mean downdraft velocity at that height. Most of the area (~ 60%) under the p_w curve is on the negative side of the w axis, indicating the higher probability of occurrence of downdrafts.

Baerentsen and Berkowicz (1984) expressed a bi-Gaussian p_w by considering the sum of two Gaussian distributions with different statistics, one for updrafts and the other for downdrafts because of their different natures of distributions as discussed above.

Luhar et al. (1996) introduced a fumigation model based on probability density function (PDF) of the random vertical velocity (w). They followed Misra's (1980) approach in developing their model.

After considering the superposition of two Gaussian distributions to approximate w PDF, first proposed by Baerentsen and Berkowicz (1984), they relaxed uniform and instantaneous mixing assumption in Misra's (1980) model. They defined values for some parameters of the bi-Gaussian PDF different from Baerentsen and Berkowicz (1984) and used simple surface reflection schemes, following Li and Briggs (1988) work. In these models key point is that positions of source–emitted particles (contaminant) in the lateral (y) and vertical (z) directions are independent and they behave as two independent random variables, at a time (t).

Luhar (2002) extended Luhar et al. (1996) PDF model by incorporating wind direction shear effects. In this work particle positions in lateral direction (y) are assumed to be varied with height and therefore also depend on (z). They treated dispersion distribution in y direction (which was the function of height z) separately and then superimposed it with bi-Gaussian PDF for vertical velocity (w) and established the new joint PDF. Although results of the model are in better agreement with field observations, however more statistical justification and validation are needed for their joint PDF.

Chapter 3

Development of a Model for an Elevated Continuous Point Source Within Convective Boundary Layer

3.1 Introduction:

A probability density function (PDF) model, to calculate the concentration profiles of pollutants from an elevated continuous point source within convective boundary layer (CBL), is derived first. Later, the fumigation model to estimate continuous shoreline fumigation is developed considering the mean structure of TIBL, analogous to mixed layer within CBL.

3.2 PDF Model For An Elevated Continuous Point Source Within Convective Boundary Layer:

A simple calculation of the ensemble-mean concentration distribution, $C(x,y,z)$, follows from mass flux considerations. The mean horizontal flux without considering the stream wise dispersion of particles through an elemental area $\Delta y\Delta z$ normal to the mean wind (U) is $UC(x,y,z)\Delta y\Delta z$. This is equal to emission rate Q times the probability of particles $p_{yz}\left((y,z;\frac{x}{U})\right)\Delta y\Delta z$ in the intervals $y-\Delta y/2<y<y+\Delta y/2$ and $z-\Delta z/2<z<z+\Delta z/2$. It can be prescribed as:

$$UC(x,y,z)\Delta y\Delta z = Q\,p_{yz}\left[y,z;\frac{x}{U}\right]\Delta y\Delta z \qquad (3.1)$$

$$C(x,y,z) = \frac{Q}{U} p_{yz}\left(y,z;\frac{x}{U}\right) \tag{3.2}$$

In the above equations it is assumed that transport by bulk motion due to mean wind in the x direction (considered as direction of wind) exceeds stream wise effective diffusion. It is commonly assumed that this condition is met for CBL when $\frac{U}{w_*} > 1.2$. In Equation (3.2), $p_{yz}\left(y,z;\frac{x}{U}\right)$ is the joint density of particle position in y and z at time t (where t is $\frac{x}{U}$). Turbulence is idealized as homogeneous and stationary. The mean wind speed (U) is assumed to be uniform with height and it does not change direction with height. The lateral and vertical velocity fluctuations are assumed to be statistically independent. In that way, the displacement of source–emitted particles in the lateral and vertical directions, y and z respectively, are independent and they behave as two independent random variables, at a time t.

So,

$$p_{yz}\left(y,z;\frac{x}{U}\right) = p_y\left(y;\frac{x}{U}\right) p_z\left(z;\frac{x}{U}\right) \tag{3.3}$$

For convenience, the source is considered at origin having the coordinates of (0,0). In the above density function it is assumed that the particle is released at the source height (z_s) at t=0.

From Equations (3.2) and (3.3)

$$C(x,y,z) = \frac{Q}{U} p_y\left((y;\frac{x}{U})\right) p_z\left((z;\frac{x}{U})\right) \tag{3.4}$$

$p_y\left(y;\frac{x}{U}\right)$ and $p_z\left(z;\frac{x}{U}\right)$ are normalized so that their integrals over all y and z equal one.

In Equation (3.4) if the density functions for $p_y\left(y;\frac{x}{U}\right)$ and $p_z\left(z;\frac{x}{U}\right)$ are assumed as Gaussian then it will end up with Gaussian plume model. But due to the skewness of vertical velocities Gaussian plume model does not work well in describing the dispersion features in the CBL. Now the task is to find the appropriate $p_y\left(y;\frac{x}{U}\right)$ and $p_z\left(z;\frac{x}{U}\right)$, which can simulate the dispersion characteristics more realistically. Weil (1988) and Weil et al. (1997) have considered $p_y\left(y;\frac{x}{U}\right)$ being Gaussian while $p_z\left(z;\frac{x}{U}\right)$ is derived from the skewed PDF, $p_w[w(z)]$, first proposed by Baerentsen et al. (1984). Weil (1988) and Weil et al. (1997) have related $p_z\left(z;\frac{x}{U}\right)$ of the particle height (z) with $p_w[w(z)]$ as;

$$p_z = p_w[w(z)]\left|\frac{dw}{dz}\right| \tag{3.5}$$

Where particle height (z) is a monotonic function of w. The relationship between w and z is found from a differential equation governing the particle trajectory:

$$w(z) = \frac{dz}{dt} \tag{3.6}$$

Where $dt = \frac{dx}{U}$

So from Equation (3.6):

$$\frac{w(z)}{U} = \frac{dz}{dx} \tag{3.7}$$

If w is independent of height, the differential equation is simply integrated to yield

$$z=z_s+\frac{wx}{U} \tag{3.8}$$

Where z_s is the source height. In the above integration it is assumed that vertical Lagrangian integral time scale T_{lz} is infinitely long, so that the particle velocity at any x (downwind distance) is uniquely determined by its value at the source. So from Equation (3.8):

$$w=(z-z_s)\frac{U}{x} \tag{3.9}$$

This is an approximation that is partially justified by the large time scales ($\frac{z_i}{w_*}\sim 10$ min) of the CBL convection elements. Weil et al. (1997) assumed that the random vertical velocity decays from its initial value w, at source, over distance inland according to $\frac{w}{f_{lz}}$.

Where $f_{lz}(x/U)$ is:

$$f_{lz}(x/U)=\left(1+0.5\frac{x}{UT_{lz}}\right)^{1/2} \tag{3.10}$$

Where

$$T_{lz}=0.7z_i/w_* \tag{3.11}$$

z_i is the boundary layer height.

After including the decay of w the trajectory Equation (3.8) would be:

$$z=z_s+\frac{wx}{f_{lz}U} \tag{3.12}$$

The convenient function f_{lz} in the trajectory Equation (3.12) satisfies both the short and long time limits of finite T_{lz}. It is assumed that vertical Lagrangian integral time scale T_{lz} is similar to the lateral Lagrangian integral time scale T_{ly}. So, the function f_{lz} is parameterized in the same way as f_{ly}. The function f_{ly} satisfies the short and long time limits of Taylor's (1921) theory (c.f. Appendix 2 for the details of Statistical theory and the finite T_{lz} behavior).

After rearranging Equation (3.12), expression for w may be given as:

$$w = (z - z_s)\frac{U f_{lz}}{x} \tag{3.13}$$

$$\frac{dw}{dz} = \frac{U f_{lz}}{x} \tag{3.14}$$

Now from Equations (3.5) and (3.14), p_z follows the expression:

$$p_z = p_w[w(z)]\frac{U f_{lz}}{x} \tag{3.15}$$

Considering the lateral dispersion as Gaussian, the probability density function of the particle position in the lateral direction p_y is:

$$p_y = \frac{1}{\sqrt{2\pi}\sigma_{yt}}\exp\left[-\frac{y^2}{2\sigma_{yt}^2}\right] \tag{3.16}$$

Putting the expressions for p_z and p_y from Equations (3.15) and (3.16) into Equation (3.4) the following expression for a continuous elevated point source with in the CBL is obtained:

$$C(x,y,z) = \frac{Q}{(2\pi)^{1/2}\sigma_{yt}x}\exp\left(-\frac{y^2}{2\sigma_{yt}^2}\right)p_w^{\Sigma} f_{lz} \tag{3.17}$$

To include reflections at the boundaries p_w values are summed up over all w values that yield significant p_w^{Σ} values (a detail description is presented in chapter 4).

Chapter 4

Development of a Shoreline Fumigation Model

4.1 Introduction:

In this chapter the PDF model developed to calculate concentration profiles in CBL is extended to coastal fumigation case. Coastal fumigation is a turbulent dispersion process in which an elevated point-source plume traveling in a stable or neutral onshore flow with relatively little diffusion is intercepted by the growing TIBL, and is subsequently mixed down to the ground by the large-scale convective eddies generated within the boundary layer.

The chapter starts by presenting the modeling work associated with spatially growing thermal internal boundary layer (TIBL). The thermal effects of the ground give rise to the development of a TIBL over land surface, during the day under onshore flow conditions. The PDF model and the parameters of the PDF model are discussed subsequently.

4.2 The Thermal Internal Boundary Layer:

Modeling of the TIBL height is a vital component of the fumigation phenomenon. The interaction between the TIBL and a plume governs the distribution of ground level concentrations (GLCs). Garratt (1992) ' zero order jump' model for the growth of the TIBL is:

$$z_i = \left(\frac{2(1+2\beta)H_f x}{\rho c_p \gamma U} \right)^{1/2} \tag{4.1}$$

Where

x is the downwind or inland distance from the land-water interface, U is an average wind speed with in the TIBL. H_f is the overland heat flux, c_p is the specific heat at constant pressure, γ is the vertical potential temperature gradient for upwind condition or above the boundary layer and β is the ratio of the downward heat flux at the TIBL to the upward heat flux at the surface; its value is approximately 0.2 for the CBL over land.

The above model is also used in CALPUFF, a meso-scale US Environmental Protection Agency (US EPA) regulatory model. In more General form:

$$z_i = A_o x^{\frac{1}{2}} \tag{4.2}$$

A_o is the function of above stated parameters (e.g. U, H_f, γ, β and c_p) and is defined as;

$$A_o = \left(\frac{2(1+2\beta)H_f}{\rho c_p \gamma U} \right)^{1/2} \tag{4.3}$$

A_o is used as an input parameter to determine the plume-TIBL interface location.

Analytical parameterizations of the thermal internal boundary-layer (TIBL) height based on the slab approach are widely used in coastal dispersion models. However, they tend to a singular behavior when the stability of the onshore flow is close to neutral. Luhar (1998) has derived a new analytical model, which is valid for neutral onshore flow conditions, as well. The present work focuses on stable onshore flow condition, which is analogous to that observed during Nanticoke fumigation experimental study. Therefore, the use of zero order jump model for the present purpose is justified. However, a minor revision is incorporated in the model. For instance, far distance downwind TIBL attains its full depth and the above stated Equation (4.2) for parabolic growth does not work. In

that situation equilibrium height z_{eq} can be given as the product of convective velocity (w_*) and convective time scale (t_*). Considering the expression for w_*, as given by Equation (1.7), and after some arrangements z_{eq} can be presented as:

$$z_{eq} = \left[\left(\frac{gH_f}{\rho c_p T_s} \right)^{\frac{1}{3}} t_* \right]^{\frac{3}{2}} \tag{4.4}$$

Where t_* is the convective time scale and its empirical value of 10 minutes is considered as suggested by Stull (1988). Subsequently, using the Equation (4.2) horizontal distance corresponding to equilibrium height can be measured.

The non-dimensional entrainment rate at the point of interception of the plume-centerline and the TIBL, (similar to Luhar et al., 1996), is expressed as:

$$\frac{w_{eo}}{w_*} = 0.5 \frac{U A_o^2}{w_* z_{io}} \tag{4.5}$$

A detailed solution is given in Appendix 1. Convective velocity (w_*) is considered to be invariant with downwind distance, as increase in the TIBL height with downwind distance is balanced by the decrease in heat flux. Their product, which seems to cause the change in w_*, does not vary strongly with downwind distance (Venkatram, 1977; Misra, 1980). Subsequently, it is also observed that variation of w_* with x makes insignificant difference in dispersion calculations when compared to those with a constant w_*.

4.3 PDF Model for an Elevated Continuous Point Source Located on Shoreline:

A tall stack situated at the shoreline, emits its pollutants into the stable layer. The plume travels with relatively little dispersion in this layer and intersects the TIBL at some distance downwind resulting into fumigation. It leads to high ground level concentrations. As discussed in Misra (1980), the dispersion of the pollutants in the stable layer and within the TIBL is considered to be proceeded independently. Now for the dispersion characteristics within TIBL the source strength is provided by the concentration field within the stable layer and the rate of growth of the TIBL. Misra(1980) assumed an elevated area source coincident with the under surface of the top of the TIBL, for the dispersion of pollutants within the TIBL. The same approach is followed by Venkatram (1988), Luhar et al. (1996) and Luhar (2002). In the present model the same source strength of pollutants for the dispersion in the TIBL is assumed.

The flux $F(x', y', z')$, from the concentration field in the stable layer to the TIBL through an infinitesimal arc AB is the sum of downward flux through CB and advective flux through AC (as shown in Figure 4.1). The source strength associated with the infinitesimal arc AB can be written mathematically as:

$$dQ(x', y', z') = K_{zs}\frac{\partial C_s}{\partial z}\Delta x'\Delta y' + U_s C_s \Delta z'\Delta y' \tag{4.6}$$

Where $z' = z_i(x')$ and $\Delta z' = \frac{dz_i(x')}{dx}\Delta x'$

Equation (4.6) can take the form:

$$dQ(x', y', z') = \left(K_{zs}\frac{\partial C_s}{\partial z} + U_s C_s \frac{dz_i(x')}{dx}\right)\Delta x'\Delta y' \tag{4.7}$$

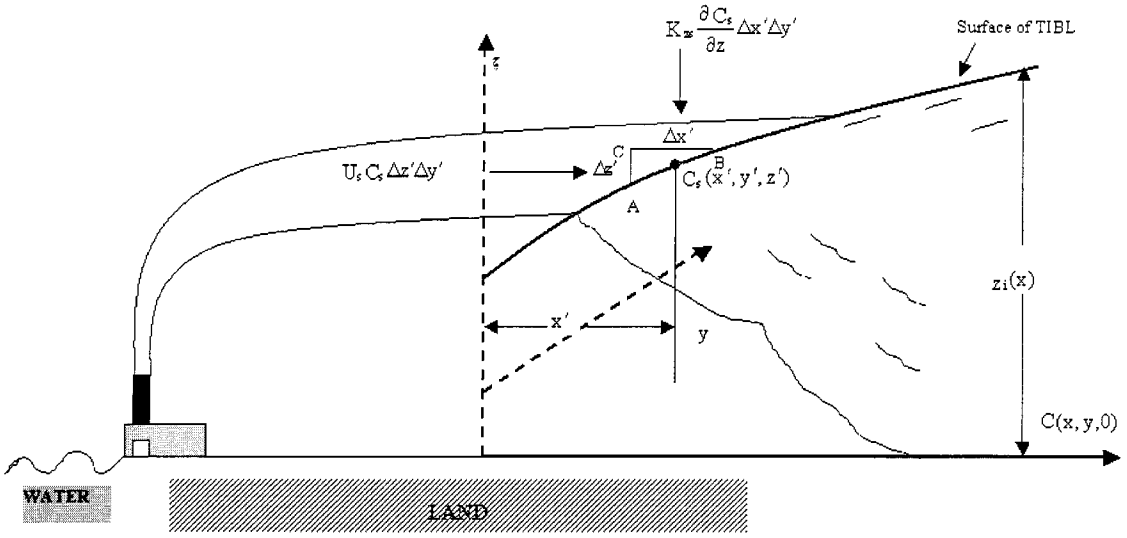

Figure 4.1 Schematic of shoreline fumigation and Geometry used to derive the expression for the ground-level concentration during fumigation

Where U_s is the wind speed in the stable layer at the height $z_i(x')$ and K_{zs} is the diffusivity coefficient in the stable layer and it can be given as:

$$K_{zs} = \frac{1}{2}\frac{d\sigma_{zf}^2}{dt} \tag{4.8}$$

In the stable layer, the distributions of velocities in both the horizontal and vertical directions are expected to be well represented by a Gaussian distribution, so do the concentrations:

$$C_s(x', y', z; H) = \frac{Q}{2\pi U_s \sigma_{yf} \sigma_{zf}} \exp\left[-\frac{(z-H)^2}{2\sigma_{zf}^2} - \frac{y'^2}{2\sigma_{yf}^2} \right] \tag{4.9}$$

It is assumed that material entrained into the TIBL cannot affect the concentration in the stable layer, so no reflection term is included in Equation (4.9).

Using Equations (4.8) and (4.9) elemental source strength can be given as (c.f. Appendix 3):

$$dQ = C_s U_s \left[\frac{dz_i(x')}{dx'} - \frac{d\sigma_{zf}}{dx'} \frac{(z_i(x') - H(x'))}{\sigma_{zf}} \right] \Delta x' \Delta y' \tag{4.10}$$

If the joint PDF for the particle position in lateral and vertical direction at time t, within the TIBL is designated as $p_{yz}\left(y, y', z; \frac{x - x'}{U} \right)$ then the concentration $dC\left(x, y, z < z_i | x', y', z_i(x)'\right)$ associated with $dQ(x', y', z_i(x)')$ (similar to Equation 3.2) can be given as:

$$dC\left(x, y, z < z_i | x', y', z_i(x)'\right) = \frac{dQ}{U} p_{yz}\left(y, y', z; \frac{x - x'}{U} \right) \tag{4.11}$$

For the same reasons as discussed earlier, the joint PDF will take the form:

$$p_{yz}\left(y,y',z;\frac{x-x'}{U}\right)=p_y\left(y,y';\frac{x-x'}{U}\right)p_z\left(z;\frac{x-x'}{U}\right) \tag{4.12}$$

Here the shape of PDF p_y is assumed as Gaussian, that is:

$$p_y\left(y,y';\frac{x-x'}{U}\right)=\frac{1}{\sqrt{2\pi}\,\sigma_{yt}}\exp\left(-\frac{(y-y')^2}{2\sigma_{yt}^2}\right) \tag{4.13}$$

The form of $p_z\left(z;\frac{x-x'}{U}\right)$ is derived from the w PDF (p_w), which is skewed and results in a non-Gaussian p_z. The relationship between the PDF of vertical position z of a particle (p_z) and the PDF of vertical velocity (p_w) is already explained and can be presented as:

$$p_z\left(z;\frac{x-x'}{U}\right)=p_w^{\Sigma}\frac{U f_{lz}}{x-x'} \tag{4.14}$$

Using Equations (4.12), (4.13) and (4.14), Equation (4.11) turns out to be:

$$dC\left(x,y,z\le z_i\middle|x',y',z_i(x)'\right)=\frac{dQ\,f_{lz}}{\sqrt{2\pi}(x-x')\sigma_{yt}}\exp\left(-\frac{(y-y')^2}{2\sigma_{yt}^2}\right)p_w^{\Sigma} \tag{4.15}$$

Where $\sigma_{yt}(\frac{x-x'}{U})$ is the crosswind spread or standard deviation within the TIBL.

Now the total concentration $C(x,y,z<z_i(x))$ due to all such sources located anywhere between 0 to x along the mean wind direction and $-\infty$ to $+\infty$ in lateral direction is obtained by:

$$C(x,y,z\le z_i)=\int dC\left(x,y,z\le z_i\middle|x',y',z_i(x)'\right) \tag{4.16}$$

After relaxing the uniform and instantaneous mixing assumption of Misra (1980) and Venkatram (1988), and by considering the variation of the plume height in the region above the TIBL prior to fumigation, the final expression is:

$$C(x,y,z<z_i(x)) = \frac{Q}{2\pi}\int_0^x \frac{f_{lz}(x,x')G(x')}{(x-x')\sigma'}\exp\left[-\frac{p^2}{2}-\frac{y^2}{2\sigma'^2}\right]p_w^{\Sigma}\,dx' \tag{4.17}$$

Where

$$p(x') = \frac{(z_i(x')-H(x'))}{\sigma_{zf}(x')} \tag{4.18}$$

$$G(x') = \frac{dp(x')}{dx'} + \frac{1}{\sigma_{zf}}\frac{dH(x')}{dx'} = \frac{1}{\sigma_{zf}}\left[\frac{dz_i(x')}{dx'} - p\frac{d\sigma_{zf}(x')}{dx'}\right] \tag{4.19}$$

$$\sigma'^2(x') = \sigma_{yf}^2(x') + \sigma_{yt}^2(x-x') \tag{4.20}$$

$H(x')$ is the plume effective height in the region above the TIBL and σ_{yf} and σ_{zf} are the dispersion spreads due to plume buoyancy in the lateral and vertical directions in the same region.

$z_i(x)$ is the TIBL height at distance where $x > x'$, σ_{yt} is the lateral dispersion spread due to the TIBL turbulence. Elemental sources are located at $z_i(x')$ at the plume-TIBL interface.

The present model is similar to that presented by Luhar and Sawford in 1996 with addition of the term f_{lz}, which accounts the effect of finite Lagrangian time scale for vertical velocities. Further, the parameters used in the present model for the calculation of p_w are obtained from Weil (1990) work and are discussed in the section 4.4.1.

4.4 PDF Model Parameters and their Significance:

4.4.1 The PDF (p_w) of the Vertical Velocity:

According to Li and Briggs (1988), the form assumed for p_w is the most important parameter for dispersion modeling in CBL. Baerentsen and Berkowicz (1984) were the first who superimposed the Gaussian distributions of vertical velocities in updrafts and downdrafts to characterize the skewed PDF (p_w) of the vertical velocity component w. Many other researchers have used the same PDF for dispersion modeling in CBL (e.g., Weil 1988, 1990; Luhar et al. 1996; Weil et al. 1997).

The generalized form of this p_w is given as:

$$p_w = \frac{\lambda_1}{\sqrt{2\pi}\,\sigma_{w1}} \exp\left[-\frac{(w-\overline{w_1})^2}{2\sigma_{w1}^2}\right] + \frac{\lambda_2}{\sqrt{2\pi}\,\sigma_{w2}} \exp\left[-\frac{(w-\overline{w_2})^2}{2\sigma_{w2}^2}\right] \tag{4.21}$$

Where λ_1 and λ_2 are weighting coefficients for the updraft and downdraft distributions respectively and their sum is 1. The $\overline{w}_j$ and σ_{wj} (j=1,2) are the mean vertical velocity and standard deviation for each distribution and are assumed to be proportional to the overall root mean square vertical turbulence velocity (σ_w). The six parameters λ_1, λ_2, $\overline{w_1}, \overline{w_2}, \sigma_{w1}$ and σ_{w2} used in the model are functions of σ_w, the vertical velocity skewness ($S = \frac{\overline{w^3}}{\sigma_w^3}$) and a parameter $R = \frac{\sigma_{w1}}{\overline{w_1}} = -\frac{\sigma_{w2}}{\overline{w_2}}$ (Weil, 1990). From the laboratory data analysis Weil et al. (1997) reported that R=1 yields fair to good agreement between the modeled and measured crosswind-integrated concentration, under strong convection. In the upper 90% of the CBL, the vertical velocity variance σ_w^2 can be considered to be

uniform (as per Weil, 1988), as can the skewness (as per Wyngaard, 1988). The expression for σ_w can be written as (Weil et al, 1997):

$$\sigma_w^2 = 1.2\,u_*^2 + 0.31\,w_*^2 \tag{4.22}$$

Where 1.2 corresponds to Hicks' (1985) neutral limit ($w_* = 0$) and the 0.31 is consistent with Weil and Brower's (1984) convective limit ($u_* = 0$) or ($\frac{\sigma_w}{w_*} = 0.56$). In the convective limit S is suggested as 0.6, which is the vertically averaged value from the Minnesota experiments (Wyngaard, 1988).

By using the above values for R, S and $\frac{\sigma_w}{w_*}$ the values for λ_1 and λ_2 turn out as 0.4 and 0.6 respectively. Luhar (2002) also parameterized the same values for λ_1 and λ_2. In another study of the bi-Gaussian PDF, Du et al. (1994) specified $\lambda_1 = 0.4$ and $\lambda_2 = 0.6$ for strong convection.

The other parameters are characterized as; $\overline{w_1} = 0.488\,w_*$, $\overline{w_2} = -0.32\,w_*$, $\sigma_{w1} = \overline{w_1}$ and $\sigma_{w2} = |\overline{w_2}|$ (c.f. Appendix 4). From these parameterizations it is evident that mean velocity of updrafts is larger then those of downdrafts.

To include reflections at the boundaries, p_w PDF should be summed over all w values that yield significant p_w values. A simple surface reflection scheme is considered here to account for the decay of w over time and to include T_{lz} effect for a skewed p_w. The revised simple reflection scheme with the inclusion of T_{lz} effect within TIBL will be:

$$w = (\pm z - z_s + 2N z_i)\frac{U f_{lz}}{(x - x')} \tag{4.23}$$

In this simple reflection scheme (after Luhar et al., 1996 and Luhar, 2002), $z_s = z_i(x')$ and $z_i = z_i(x)$ are assumed, thus Equation (4.23) transforms to:

$$w = \left((\pm z - z_i(x') + 2N z_i(x))\right)\frac{U f_{lz}}{(x - x')} \tag{4.24}$$

Where N is any integer; and $|N|$ is the number of times that reflection from z_i occurs. For calculating the ground level concentration (GLC) i.e. ±z=0, the term +z=0 and -z=0 should be used to calculate w in the above expression. The direct trajectory is represented by N=0. A value of parameter $|N|$ up to 4 is significant for the GLC calculations at distance far downwind from the source.

Finally, the vertical velocity (w) PDF in the summation form is given as:

$$p_w^{\Sigma} = \sum_{k=-N}^{N}\sum_{j=1}^{2}\frac{\lambda_j}{\sqrt{2\pi}\,\sigma_{wj}}\left[\exp\left[-\frac{(w_1 - \overline{w_j})^2}{2\sigma_{wj}^2}\right] + \exp\left[-\frac{(w_2 - \overline{w_j})^2}{2\sigma_{wj}^2}\right]\right] \tag{4.25}$$

Where

$$w_1 = \left((+z - z_i(x') + 2k z_i(x))\right)\frac{U f_{lz}}{(x - x')} \tag{4.26}$$

$$w_2 = \left((-z - z_i(x') + 2k z_i(x))\right)\frac{U f_{lz}}{(x - x')} \tag{4.27}$$

4.4.2 Expressions for Plume Rise and Vertical and Lateral Dispersion Coefficients in Stable Layer:

The plume's internal turbulence buoyancy controls the dispersion in onshore stable flows of plumes from tall stacks, prior to fumigation (for e.g. Misra and McMillan, 1980; Briggs, 1984; Lahur et al 2002).

Final rise of a buoyant plume dispersing in a stably stratified environment according to Briggs' (1984) expression is:

$$z'_{eq} = 2.6[F_o/(UN_e^2)]^{\frac{1}{3}} \tag{4.28}$$

Where N_e is layer's natural frequency in stable boundary layer (SBL), known as Brunt-Vaisala frequency. Buoyancy waves that propagate upward within the SBL eventually reach a level where their frequency matches the ambient Brunt-Vaisala frequency, at which point they reflect back down toward the ground. N_e is given as;

$$N_e = [g\gamma/T_a]^{\frac{1}{2}} \tag{4.29}$$

γ = Change of potential temperature with height [K/m].

T_a = Ambient temperature [K].

F_o = Buoyancy flux = $\frac{gv_s D_s^{\,2}(T_{gs} - T_a)}{4T_a}$ [m^4/Sec^3].

T_{gs} = Gas Temperature at stack exit [K].

D_s = Inside diameter of the stack exit [m].

As long as the buoyant plume has a temperature excess over the surrounding atmosphere, the plume will continue to rise. For buoyant plumes, this transitional plume rise is estimated, as presented by Briggs (1972).

$$z'_n = 1.6F_o^{\frac{1}{3}}x^{\frac{2}{3}}U^{-1} \tag{4.30}$$

Comparing Equations (4.28) and (4.30) the distance where final plume rise is achieved can be determined as:

$$x_f = 2.07UN_e^{-1} \tag{4.31}$$

So the plume rise Δh can be defined at some downwind distance as z'_n (if $z'_n < z'_{eq}$) otherwise z'_{eq}.

If the distance where lower portion of the plume intersects the TIBL is less than x_f then Misra's (1980) parameterization for the term $G(x')$ is used in the present model equation i.e. the term $\frac{dH(x')}{dx'}$ becomes zero in Equation (4.19). Otherwise in the case where the buoyant plume in the region above the TIBL changes height prior to fumigation, the above formulation given in Equation (4.19) will be considered (c.f. Appendix 3).

When the plume's internal turbulence generated by buoyancy, dominates plume dispersion in a non-turbulent environment then according to Briggs (1984), plume radius grows as:

$$r = \beta_1 z'_n \tag{4.32}$$

Where β_1 (0.4-0.6) is an entrainment parameter.

Luhar et al. (2002) assumed the spread of the plume as:

$$r/\sqrt{2} = 0.35 z'_n \tag{4.33}$$

Considering the Equation (4.33) coupled with the influence of the stable stratification, after Luhar et al. (2002), the vertical dispersion parameter σ_{zf} can be expressed as:

$$\sigma_{zf} = 0.35\Delta h \tag{4.34}$$

The lateral dispersion coefficient, which is not influenced by the stable stratification, is given as:

$$\sigma_{yf} = 0.35 z_n' \tag{4.35}$$

4.4.3 Expression for Lateral Dispersion Coefficient within TIBL:

The lateral dispersion in TIBL is assumed to be dominated by ambient turbulence. This lateral spread is parameterized by the general form (e.g. Venkatram 1988, Weil 1988, Luhar et al. 2002):

$$\sigma_{yt} = \sigma_v t \left(1 + \frac{0.5t}{T_{ly}}\right)^{-\frac{1}{2}} \tag{4.36}$$

Weil et al. (1997) presented the following expression for the lateral velocity variance as:

$$\sigma_v^2 = 3.6 u_*^2 + 0.31 w_*^2 \tag{4.37}$$

Although Draxler (1976) suggested a value of 500s for T_{ly}, however here its value is adopted as $T_{ly} = 0.7 z_i / w_*$ following Weil and Corio (1985). From the above discussion and also considering Weil and Brower's (1984) convective limit ($u_* = 0$), Equation (4.36) takes the form in the present model as:

$$\sigma_{yt}(x, x') = \frac{0.56 w_* (x - x')}{U f_{ly}} \tag{4.38}$$

Where

$$f_{ly}(x, x') = \left[1 + \frac{0.5(x - x')}{U T_{ly}}\right]^{\frac{1}{2}} \tag{4.39}$$

This function satisfies the short and long time limits of statistical theory and takes care of the finite lateral Lagrangian time scale (c.f. Appendix 2).

4.4.4 Vertical Dispersion within TIBL:

Within the TIBL, dispersion of particles occurs in updrafts and downdrafts. The distribution characteristics and strength of updrafts and downdrafts in the CBL are different. Lamb (1982) reported that turbulent energy in updrafts is higher than in downdrafts. It is also understood that the mean velocity of updrafts is larger than downdrafts. So vertical dispersion of plume particles depend on their presence in updrafts or downdrafts. If it is considered that vertical Lagrangian time scale is infinite then vertical dispersion is given by:

$$\sigma_{zj}(x,x') = \sigma_{wj}\frac{x-x'}{U} \tag{4.40}$$

Where j=1,2 is representing updraft and downdraft respectively. After considering the decaying factor $f_{lz}(x,x')$ for vertical velocity and by taking the finite Lagrangian scale into account, vertical dispersion term becomes (c.f. Appendix 2):

$$\sigma_{zj}(x,x') = \sigma_{wj}\frac{x-x'}{Uf_{lz}} \tag{4.41}$$

Where

$$f_{lz}(x,x') = \left[1+\frac{0.5(x-x')}{UT_{lz}}\right]^{\frac{1}{2}} \tag{4.42}$$

After Weil et al. (1997), T_{lz} is considered as $T_{lz} = T_{ly} = 0.7z_i / w_*$. This shows good agreement of results with observed data for the Nanticoke power plant (discussed in Chapter 5).

In Equation (4.41) the term $f_{lz}(x,x')$ will push the point of maximum concentration further down wind, because the vertical dispersion reduces by incorporating that term. At large distances even this effect will be more pronouncing, that is little dispersion. But there will be more plume to be dispersed at large distances. The effect of finite Lagrangian time scale is presented in Figure 4.2. In finite T_{lz} case, the concentration is lower for small distances and higher for large distances than those for infinite T_{lz}. This can be attributed with the reduced vertical dispersion initially, causing more plume material to get dispersed at long tails, with the inclusion of finite T_{lz}.

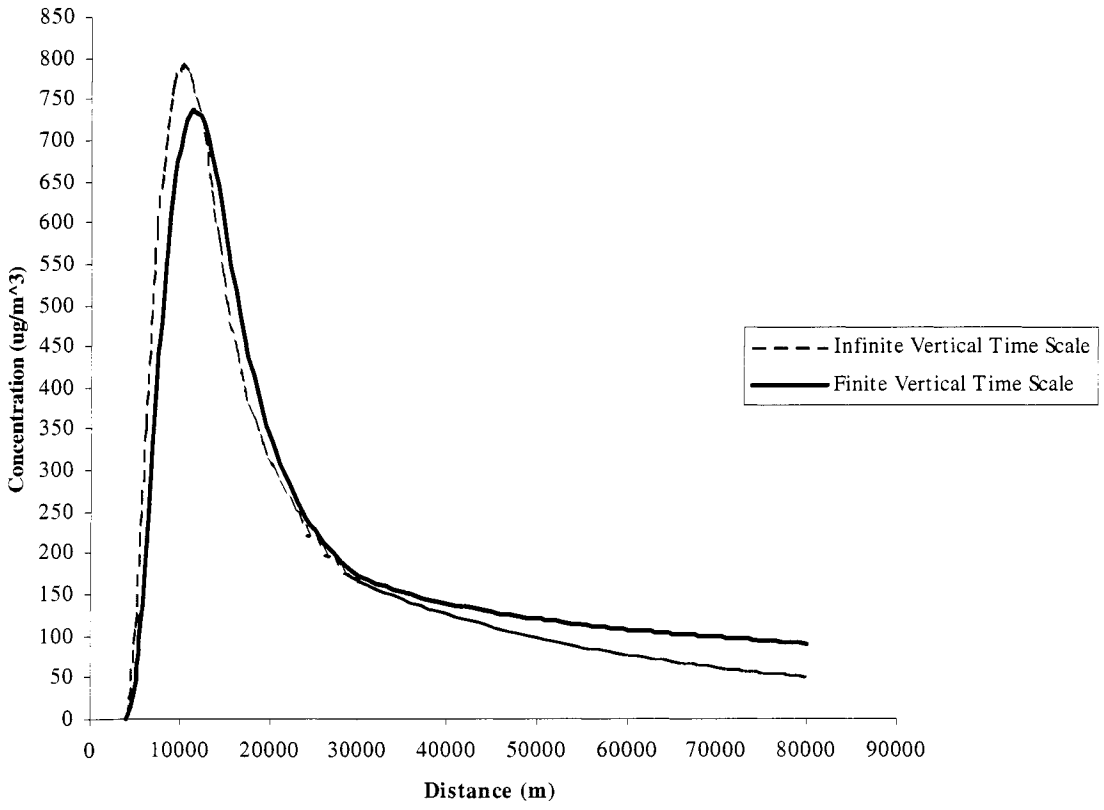

Figure 4.2 Effect of finite vertical Lagrangian time scale

Chapter 5

Model Testing and Validation

5.1 Introduction:

Several field and laboratory experiments have been undertaken to characterize the phenomenon of coastal fumigation. One of the most comprehensive coastal dispersion experiments, was conducted at Nanticoke during May 29 to June 16, 1978, designated hereafter as EXP I. The results of this study would be used to carry out performance evaluation of current model.

This chapter reviews the experimental program (EXP I) in a brief and describes a framework to evaluate the performance of air quality model. Statistical analysis of the current model and its comparison with the two previous studies based on the models of Misra (1980) and Luhar et al. (1995) are also presented.

5.2 Experimental Program:

EXP I, carried out by the Atmospheric Environment Service (AES) of Environment Canada in cooperation with the Ontario Ministry of the Environment (OME) and Ontario Hydro, was commenced to obtain detailed meteorological measurements of the vertical structure of onshore flows, boundary layer development and surface and airborne pollutant measurements during fumigation conditions.

Nanticoke is situated on the northern shore of Lake Erie. The electric power generating station of Ontario Hydro at Nanticoke has two 198 m stacks separated by 273 meters. This coal-fired power plant has a generating capacity of 4000 MW. At design full load (4000 MW) and using coal containing 2.3% sulfur, emission of SO_2 of magnitude of 16

kg/s is expected from both stacks (Misra at el. 1982). During the field experiments the SO_2 emission rate remained at about 5 kg/s.

Many systems, including tethersonde, minisonde, acoustic sounder and sonic anemometers, were deployed to measure the height and structure of both the TIBL as a function of inland distance during onshore flow and the stable layer aloft.

A LIDAR unit, operated from a mobile van, was used to measure plume rise, plume bearing and its dispersion characteristics as a function of downwind distance. Three correlation spectrometers (COSPEC) were mounted in three different vehicles. The two COSPEC vehicles also had Sign-X SO_2 monitors to obtain the ground level distribution of SO_2 simultaneously with the overhead SO_2 burden while traversing. Fixed ground level Philips SO_2 monitors and mobile chemistry laboratories augmented these data sets. A helicopter and an aircraft platform were also used to measure SO_2.

During the study period, gradient or lake breeze flows transported the Nanticoke power plant plume inland only on 8 days: 29, 30 May; 1, 4, 6, 12, 15 and 16 June (Portelli, 1982). Two days, June 1 and 6, 1978, were selected for comprehensive presentation as data coverage was considered better than on other days and two noticeably different fumigations existed.

On the 1st June light gradient flow allowed for a lake breeze, which veered with time of day resulting in a systematic clockwise rotation of the fumigation zone. On the 6th June relatively fixed fumigation was reported during steady gradient onshore flow.

5.3 Model Testing and Validation Methodology:

Venkatram (1982) described a framework to evaluate air quality model predictions against observations. He proposed the following relationship between observations and predictions from a model

$$\hat{C}_o(x_1, x_2) = \hat{C}_p(x_1) + \varepsilon(x_2) \tag{5.1}$$

Where $\hat{C}_p(x_1)$ represents the predicted values, which are the functions of inputs (x_1) used in model, x_2 denotes unknown variables, which affect the observed concentration $\hat{C}_o$ and $\varepsilon(x_2)$ is designated as residual which is due to unknown variables not included in the model. The observation term $\hat{C}_o(x_1, x_2)$ is made up of a deterministic component, $\hat{C}_p(x_1)$, as well as stochastic part, $\varepsilon(x_2)$. In the above equation it is assumed that inputs to model and observed values are error free.

Venkatram (1982) recommended the natural log transformation of the observed and predicted concentration values (i.e. $\hat{C} = \ln C$) to get the normally distributed residuals. Here it is proposed that before any transformation of observed and predicted data residuals should be checked for normality. If residuals are not normally distributed then take logarithm of both samples, and use differences of logarithm. This fact is obvious from Figure 5.1. Residuals are normally distributed with out any prior transformation of observed and measured data. Standard deviation (SD) of residuals determines the expected deviation about its mean value. A small standard deviation is desired about the mean. This confirms little variability in measurements by the model about the mean value.

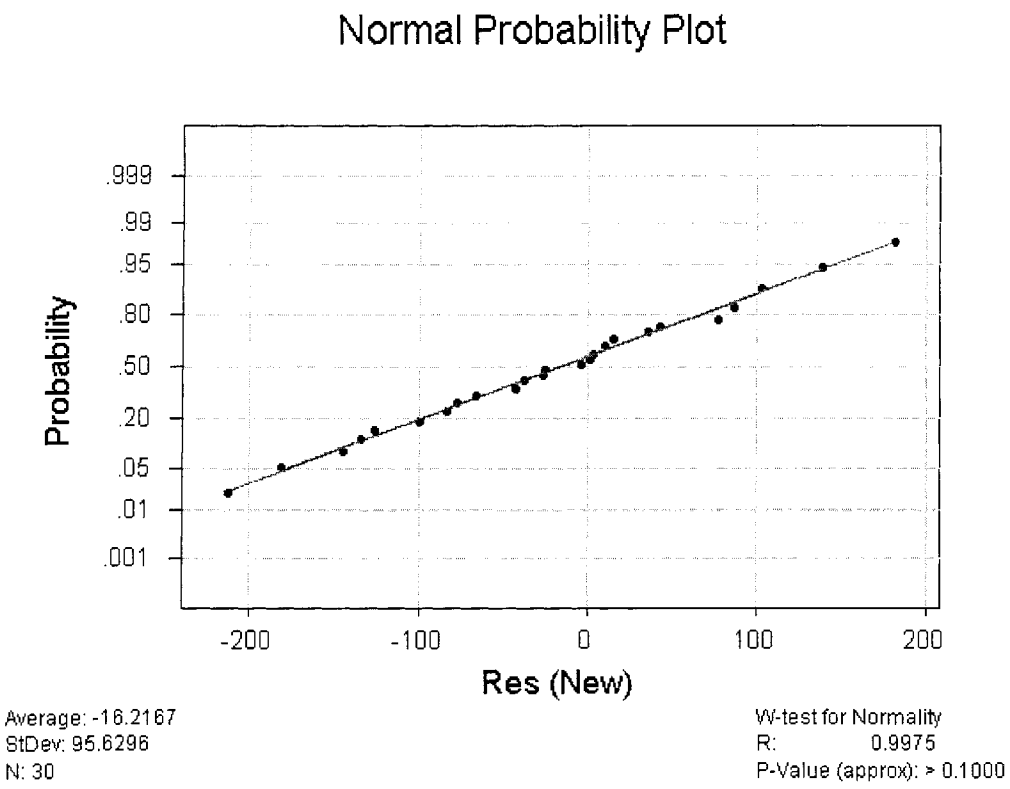

Figure 5.1 Normal probability plot for Residuals

A residual analysis, where magnitude of an arithmetic mean is zero or near to zero and magnitude of geometric mean (in case of log transformation) is 1 or near to 1 but having large standard deviation does not ensure the good performance of the model. On the other hand a residual analysis, where ideal mean value is not achieved but it is having small standard deviation, can perform more effectively. So, in the current study mean absolute error (MAE) and mean relative error (MRE) for residuals are also used as quantitative measures besides mean and standard deviation. Mean absolute error is reported as:

$$MAE=\frac{1}{N}\sum_{i=1}^{N}|\varepsilon| \tag{5.2}$$

Mean relative error is defined as:

$$MRE(\%)=\frac{100}{N}\sum_{i=1}^{N}\frac{|\varepsilon|}{C_o} \tag{5.3}$$

Where N represents the sample size.

ε is given as:

$$\varepsilon=C_o-C_p \tag{5.4}$$

C_o and C_p represent the observed and predicted concentrations respectively.

So a model having the lower values of standard deviation of residuals, MAE and MSE should show good performance. Moreover, the condition that ε is independent of input variables x_1, should be fulfilled (Venkatram, 1982). From Draper and Smith (1981), if ε is not a function of x_1 the plot should look like a band distributed around $\varepsilon=0$.

5.4 Solution of the Model Equation and Validation of Results:

The quantity x' in the model is an integration variable that corresponds to the location of an elemental source, at the plume-TIBL interface, between 0 and receptor location x. Each source will contribute some concentration at location x. The total concentration is found at x by summing up all these contributed concentrations through the method of integration. All of these elemental sources will lie in the fumigation zone, anywhere between 0 and x.

The fumigation zone starts where the lower end of the plume touches the TIBL and ends where its upper layer intercepts the TIBL. The height at which centerline of the plume intercepts the TIBL may be given as:

$$z_{io} = h_s + \Delta h \tag{5.5}$$

Where h_s is the physical stack height.

Δh is the plume rise as already discussed in section 4.4.2.

The corresponding horizontal distance may be given by using the Equation (4.2) as:

$$x_{io} = \left[\frac{z_{io}}{A_o}\right]^2 \tag{5.6}$$

The vertical dispersion of the plume is Gaussian within the stable region. Approximately 95 percent of the plume material will be laying within 2 times the standard deviation about the mean. So, the height which corresponds to the start of the fumigation zone (z_{fs}), is given by the following expression:

$$z_{fs} = z_{io} - 2b\sigma_{zfo} \tag{5.7}$$

Where b=0.7 is obtained from a laboratory study of the fumigation phenomenon, carried out by Hibberd and Luhar (1996). However, the vertical variability in the local TIBL height during the one-hour averaging time is considered negligible.

σ_{zfo} is the vertical dispersion coefficient in the stable layer corresponding to horizontal distance (x_{io}).

Similarly, expression for the height corresponding to the ending of the fumigation zone is:

$$z_{fe} = z_{io} + 2b\sigma_{zfo} \tag{5.8}$$

The horizontal distance at which the fumigation zone starts is calculated by the following expression:

$$x_{fs} = \left[\frac{z_{fs}}{A_o}\right]^2 \tag{5.9}$$

The ending distance of the fumigation zone is expressed as:

$$x_{fe} = \left[\frac{z_{fe}}{A_o}\right]^2 \tag{5.10}$$

The parameters being used as input to the model include: temperature, effective wind speed, convective velocity w_*, a parameter A_o to predict the growth of TIBL, effective Brunt-Vaisala frequency (N_e) of onshore flow and emission rate. These parameters are obtained from Kerman et al. (1982) and Misra et al. (1982) and are presented in Table 5.1.

The final plume rise is calculated for each stack and mean rise is calculated by taking the average of them by assuming the same loading on each stack. The plume achieves the final rise before its lower portion starts touching the TIBL.

Model i.e. Equation (4.17) is solved by coding in MATLAB 6.5 (c.f. Appendix5). Within the fumigation zone 51 source points at the Plume-TIBL interface are considered between 0 to x. The concentrations contributed by these 51 source points (50 panels) at receptor x are summed up through integration to get the total concentration at x. In MATLAB this integration is done with the trapz function, which implements the trapezoidal rule of integration.

To check the accuracy of the results the number of source points increased to 501 (500 panels). A comparison of concentration results between 50 and 500 panels shows that the maximum relative error at any distance downwind is approximately 0.7% (parts per billion) and is considered negligible. Hence, by trial 51 source points give satisfactory convergence to the true solution for any distance downwind.

Under the meteorological conditions, prevalent during the Nanticoke experiment, the running time was 4 seconds with 50 panels for simulating the results between 0 to 80000 meters with the grid spacing of 1000 meters (Pentium Pro III, 550 MHz processor). However, under the similar set of conditions with 500 panels the running time increased to 20 seconds.

Results obtained from the current model, Misra's (1980) model, Lagrangian stochastic model from Luhar et al. (1995) and field observations from Misra et al. (1982) are presented in Table 5.2.

Table 5.1 Model Inputs

Day-hr	Horizontal Distance (km)	Lateral Distance (km)	U/w*	w* (m/sec)	A_o ($m^{1/2}$)	Brunt-Vaisalla frequency (sec^{-1})	Buoyancy Flux (m^4/s^3) S1*	S2**	Avg+	Emission Rate (Kg/s)
1—11	16.4	-1	3.67	1.28	4.95	0.017	564	1053	808.5	6.55
	10	0								
	8	-0.5								
1—12	16	0	3.88	1.29	4.66	0.0144	448	1059	753.5	6.25
	16	1.5								
1—13	15.9	0	3.41	1.38	4.4	0.0176	448	950	699	6.03
	15.4	-0.5								
	15.4	-1								
1—14	15.9	0	4.38	1.28	3.95	0.0192	448	950	699	5.59
	16.1	-0.2								
	16.1	-0.5								
1—15	15.9	0	4.79	1.17	3.56	0.0249	528	949	738.5	5.09
	14.3	0								
	14.3	-0.5								
6—12	14.5	-0.5	5.68	1.32	3.16	0.0188	448	582	515	4.2
6—14	14.2	0	5.05	1.21	2.71	0.0246	448	802	625	5.07
	14.2	-0.5								
	8	-0.5								
6—15	8	0.25	3.97	1.47	5.27	0.013	448	972	710	5.76
	8	-0.25								
	8	0.5								
	8	-0.5								
	14.5	0.5								
	14.5	-0.5								
	14.5	1								
	14.5	-1								
6—16	8	0	4.35	1.47	5.6	0.0092	527	875	701	6.03
	14.5	-0.4								
6—17	14.5	-0.5	5.93	1.17	4.5	0.01	271	500	385.5	5.52
	14.5	-1								
	14	0								

* Buoyancy Flux from Stack 1

** Buoyancy Flux from Stack 2

+Average Buoyancy Flux

Table 5.2 Predicted and Observed Concentrations

Day--hr	Horizontal Distance (km)	Lateral Distance (km)	C_p (ppb) Misra's Model	C_p (ppb) Luhar's Lagrangian Model	C_p (ppb) PDF New	C_o (ppb) Observed
1--11	16.4	-1	124	179.4	187	87
	10	0	590	351.4	476	410
	8	-0.5	276	219.1	234	250
1--12	16	0	435	307.6	369	243
	16	1.5	23	100.8	61	243
1--13	15.9	0	437	246.2	389	400
	15.4	-0.5	308	276.03	330	185
	15.4	-1	118	211.42	184	185
1--14	15.9	0	422	311.1	397	400
	16.1	-0.2	335	335	378	165
	16.1	-0.5	237	245	300	165
1--15	15.9	0	382	264.4	399	217
	14.3	0	287	322.4	400	363
	14.3	-0.5	177	167.2	285	363
6--12	14.5	-0.5	189	58.9	134	145
6--14	14.2	0	160	163.64	191.5	114
	14.2	-0.5	92	115.8	118	114
	8	-0.5	31	36	0	36
6--15	8	0.25	436	403	268	355
	8	-0.25	436	403	268	355
	8	0.5	180	217.2	161	355
	8	-0.5	180	217.2	161	355
	14.5	0.5	243	213	251	78
	14.5	-0.5	243	213	251	78
	14.5	1	26.4	164.4	121	78
	14.5	-1	26.4	164.4	121	78
6--16	8	0	696	273.8	221	710
	14.5	-0.4	288	147.8	234	209
6--17	14.5	-0.5	267	210	216	190
	14.5	-1	60	70	51	190
	14	0	488	303	357	400

5.5 Statistical Analysis and Discussion:

For the performance evaluation of a model the inputs to a model and observed values should be free of error. It is evident from Misra et al. (1982) that due to an accuracy of $\pm 5^{o}$ in the measurement of wind direction, the crosswind position of monitors was determined within an accuracy of 500-1500m. Also, source emission rates were not measured during the field experiments rather they were determined from a mass balance analysis. However during the current analysis all the observations are considered as free of error except the reading observed at 1600 hours on the 6th June. The magnitude of 710 ppb had not been observed at any other time or day, even though at 1500 and 1600 hours on the 6th June, the lateral plume spreads and convective velocity were approximately the same and emission rates were also not considerably different.

Instead of running the model for average input values for some specific hours as done by Luhar et al. (1995), here the model is run separately for each hour. The Model is very time efficient and running time was less then 5 seconds (Pentium Pro III, 550 MHz processor). From Table 5.1 the stability index of $\frac{U}{w_*}$ remains below 6, which shows the strong convection regime during experiments.

The Probability plot of residuals for PDF model is plotted and checked for normality without any transformation. From Figure 5.1 it's evident that Residuals pass the normality test.

The other quantitative measures discussed above are reported in Table 5.3. Here the residuals are in the unit of parts per billion (ppb).

In this scenario there are two major sources of uncertainty, which are impediment in performance evaluation of the model. The first source is related to the uncertainty of data measurement. As mentioned above the error involved in the measurement of wind direction causes the uncertainty in cross wind locations of SO_2 monitors. Also improper sampling time causes this kind of uncertainty in the concentration measurements. The second source of uncertainty can be categorized as statistical uncertainty. This uncertainty evolves due to less number of observations and is resulted due to budget and time constraints.

Standard deviation of residuals (SD) and Mean standard error (MAE) are minimum for the results obtained from present model. To check for the constant variance of residuals plots are drawn between residuals and predicted values in Figures 5.2 (a to c).

It is evident from the analysis of residual plots, for the present model the residuals are more uniformly distributed about zero line than those of the models presented by Luhar and Misra. The dispersion of residuals about zero residual line is minimum for the present model. Moreover residual plot is showing nice scatter for present model, without any funnel shape, confirming the constant variance.

Figures 5.3 (a to d) show residual plots against the input parameters for present model. The distributions of residuals are in bands showing that residuals are independent of model inputs.

Table 5.3 Quantitative measures of coastal dispersion model performance

Model	Summary Measures			
	Mean	SD	MAE	MRE (%)
Misra's Model	-23	117.8	100.3	55
Stochastic Model (Luhar et al. 1995).	5.6	99.4	84.43	49.5
Present Model	-16.2	95.6	76.35	46.4

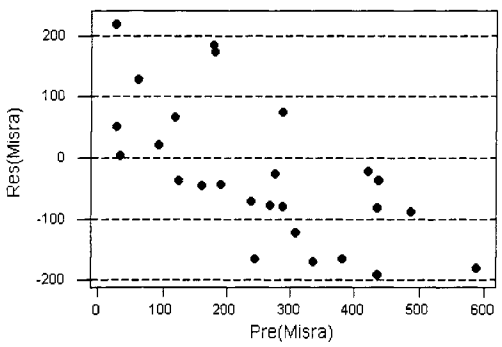

(a) Misra's Model

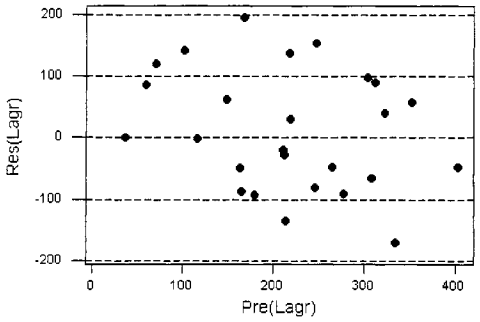

(b) Lagrangian Model

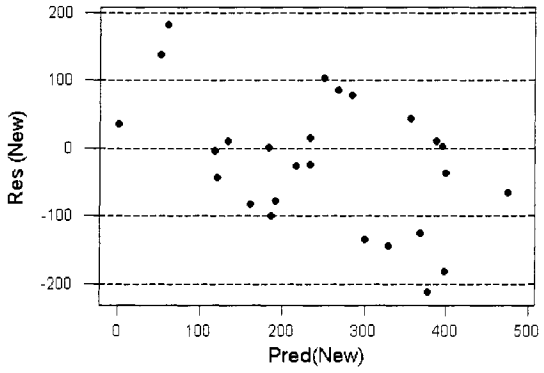

(c) Present Model

Figure 5.2 Plot of residuals (ppb) against predicted concentration values (ppb)

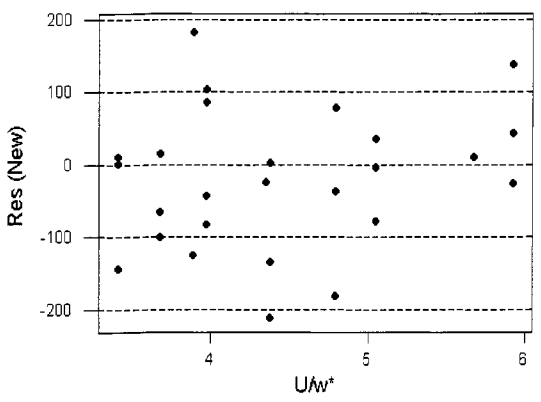

(a) Residuals against ratio of mean wind speed to convective velocity

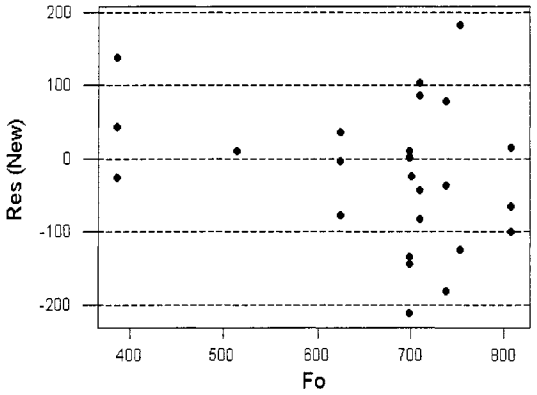

(b) Residuals against buoyancy flux

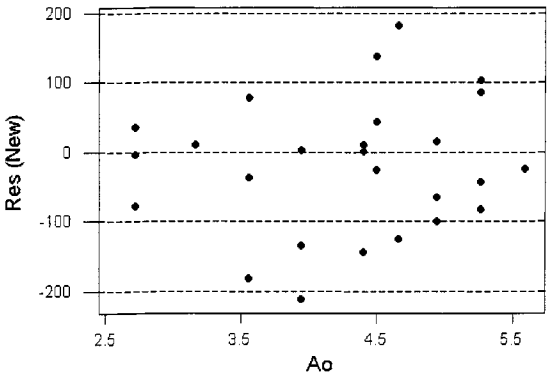

(c) Residuals against A_o

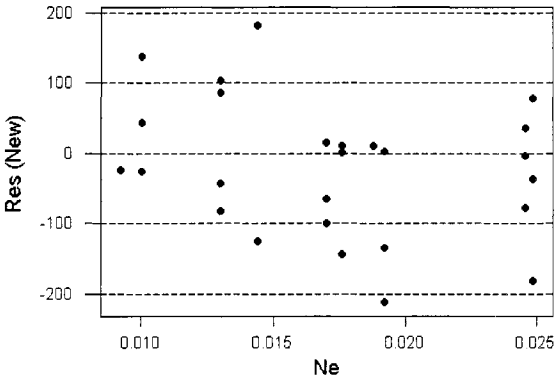

(d) Residuals against Brunt-Vaisalla frequency (N_e)

Figure 5.3 Plot of residuals (ppb) against model inputs for the new model

Chapter 6

Sensitivity Analysis

6.1 Introduction:

In this chapter sensitivity analysis of the base model has been carried out. Sensitivity analysis is used widely as a tool to examine the impact of the model input data on the results. The objective of sensitivity analysis is to identify the critical variables that have significant influence on the model results. An evaluation of these critical variables helps in quality assurance of input data as well as results.

6.2 Sensitivity Analysis of Model Input Parameters:

The input variables to the model are characterized in two groups: i) source parameters and ii) meteorological parameters. In evaluation a segmental % increase / %decrease (from the mean value) is given in one parameter while maintaining other input variables to their mean values.

The variables considered for sensitivity analysis and associated results are discussed here.

6.2.1 Sensitivity Analysis of The Ratio $\frac{U}{w_*}$:

The parameter (convective velocity) w_* is used as a scaling parameter in the convective boundary layer. It is categorized as a meteorological parameter. The ratio of mean wind speed to convective velocity i.e. $\frac{U}{w_*}$ serves as a stability index and is used to distinguish between strong and weak convective regimes. For the strong convective regime condition

this ratio should be less than 6. Moreover to avoid stream wise diffusion the ratio should be greater than 1.2 (Weil, 1988).

To carry out sensitivity analysis, the mean value of the ratio is considered as 3.5. The maximum increase in the value by 50% and maximum decrease by 50% give magnitudes of 5.25 and 1.75 respectively and are well within the limits of $1.2 < \frac{U}{w_*} < 6$ for the model use. The other magnitudes of $\frac{U}{w_*}$ corresponding to both 25% decrease and increase and maximum concentrations (C_{max}) and corresponding horizontal distances from the stack (X_{max}) are shown in Table 6.1. The % increase or decrease in C_{max} and X_{max} from the mean values is also shown in Table 6.1.

Table 6.1 Model Sensitivity to the parameter U/w_*: maximum concentrations and corresponding distances

U/w_*	% Difference from the mean value	C_{max} ($\mu g/m^3$)	X_{max} (m)	% Difference of C_{max} from the concentration corresponding to mean value	%Difference of X_{max} from the distance corresponding to mean value
1.750	-50.00	1390.00	5500.00	-14.83	-21.43
2.625	-25.00	1540.00	6000.00	-5.64	-14.29
3.500	0.00	1632.00	7000.00	0.00	0.00
4.375	25.00	1684.00	7500.00	3.19	7.14
5.250	50.00	1709.00	8000.00	4.72	14.29

Note: (-) sign shows the decrease from the mean value.

An increase in w_* value implies increased heat flux and plume instability due to convection. This means that lower values of $\frac{U}{w_*}$ cause more of a cross wind dispersion thus reducing overall ground level concentrations and moving the maximum

concentration location closer to the stack. This fact is mathematically evident from Equation (4.38), which is used in the model to calculate TIBL crosswind dispersion coefficient (σ_{yt}). Consequently, higher values of $\frac{U}{w_*}$ cause little crosswind dispersion resulting higher concentrations.

It is obvious from Figure 6.1 that the physical reasoning related to the effect of $\frac{U}{w_*}$ on distribution holds true. Table 6.1 shows that the largest value $\frac{U}{w_*}$ of 5.25 corresponds to both the highest concentration value (1709 $\mu g/m^3$) and the farthest downwind peak (8000 m). This demonstrates that the plume is not as dispersed as for the smaller ratios and is advected comparatively farther downwind.

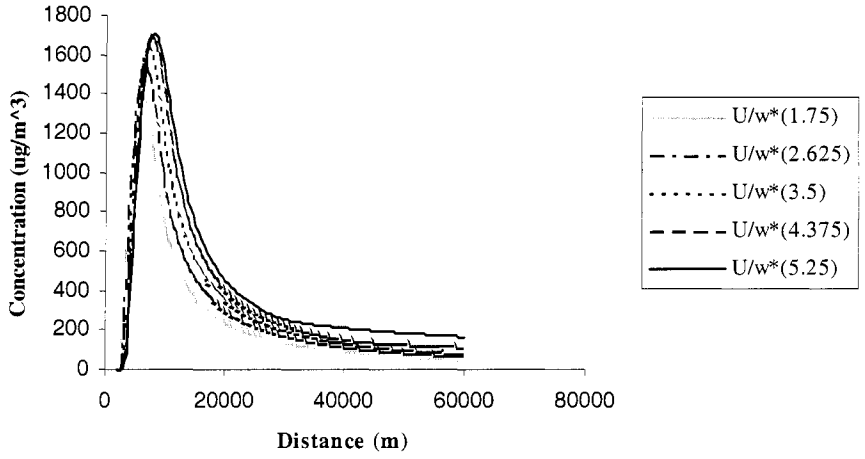

Figure 6.1 Model sensitivity to the parameter $\frac{U}{w_*}$

6.2.2 Sensitivity Analysis of Parameter A_0 :

A sensitivity analysis on the factor A_0 represents the effect of the TIBL height variations on model outputs. It includes the information necessary for computation of the TIBL

height and is given by expression (4.3). As this parameter depends on other meteorological parameters so it is characterized as a meteorological parameter.

Higher values of A_o in Table 6.2 correspond to steep TIBL. A steep TIBL results in high concentrations with peaks close to the source and within a short fumigation zone. This is presented in Figure 6.2. A comparison of maximum concentrations and their locations is given in Table 6.2.

Table 6.2 Model Sensitivity to the parameter A_o: maximum concentrations and corresponding distances

A_o ($m^{1/2}$)	% Difference from the mean value	C_{max} ($\mu g/m^3$)	X_{max} (m)	% Difference of C_{max} from the concentration corresponding to mean value	%Difference of X_{max} from the distance corresponding to mean value
2.00	-50.00	807.00	22000.00	-50.55	214.29
3.00	-25.00	1262.00	10500.00	-22.67	50.00
4.00	0.00	1632.00	7000.00	0.00	0.00
5.00	25.00	1850.00	5000.00	13.36	-28.57
6.00	50.00	1923.00	4000.00	17.83	-42.86

Note: (-) sign shows the decrease from the mean value.

Concentration curve resulted from the steepest TIBL ($A_o = 6$) goes up sharply. Lesser values of A_o or shallow TIBLs decrease the magnitude of maximum concentration and push its location further downwind. Also plume travels far downwind in shallow TIBL due to TIBL suppression. This fact is shown by the curve for the smallest A_o value of 2; where concentration levels are higher than other cases at distances far downwind.

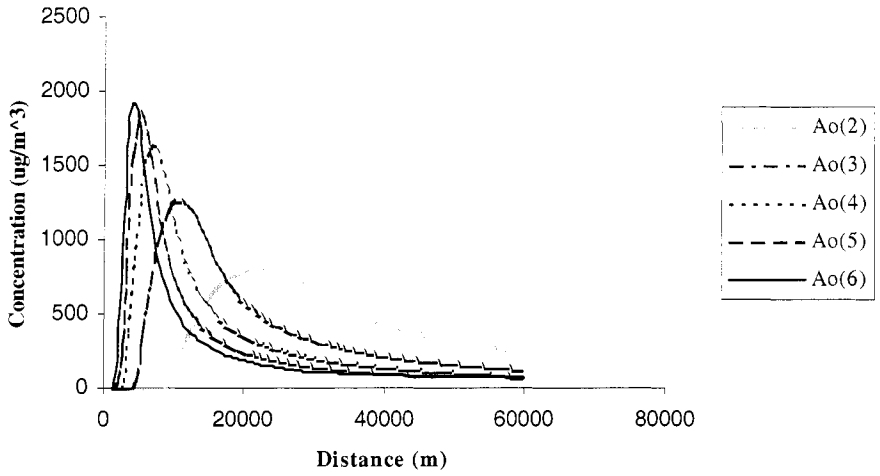

Figure 6.2 Model sensitivity to the parameter A_o ($m^{1/2}$) (TIBL Model parameter)

6.2.3 Sensitivity Analysis of Parameter N_e :

Brunt-Vaisalla frequency (N_e) is used to quantify the stability of the stable air. N_e is layer's natural frequency in stable boundary layer. This parameter depends on the properties of marine air. A buoyant effluent that has reached its equilibrium height within stable boundary layer will oscillate with this natural frequency and will only dependent on the properties of air. Higher value of N_e corresponds to strong thermally stratified onshore flow and strong inversion. This results in plume suppression because of increased marine air stability and plume will impinge TIBL at small horizontal distance moving the highest ground level concentration value towards the stack. Also the plume has less dispersion in the stable air and impacts TIBL with higher concentrations. Decreasing the value of N_e aids in the plume rise. The plume will travel within the stable layer comparatively far distance downwind before entrapping into TIBL, thus moving the maximum ground level concentration away from the source. Also the increased

dispersion of the plume in the stable air would reduce the maximum ground level concentration after plume impaction. A quantitative comparison of maximum concentrations and their location at various N_e values is given in Table 6.3.

Figure 6.3 also supports the above stated physics of plume dispersion associated with the parameter N_e.

Table 6.3 Model Sensitivity to the parameter N_e: maximum concentrations and corresponding distances

Ne (Sec^{-1})	% Difference from the mean value	C_{max} ($\mu g/m^3$)	X_{max} (m)	% Difference of C_{max} from the concentration corresponding to mean value	%Difference of X_{max} from the distance corresponding to mean value
0.010	-50.00	759.00	11000.00	-53.49	57.14
0.015	-25.00	1205.00	8500.00	-26.16	21.43
0.020	0.00	1632.00	7000.00	0.00	0.00
0.025	25.00	2038.00	6000.00	24.88	-14.29
0.030	50.00	2406.00	5500.00	47.43	-21.43

Note: (-) sign shows the decrease from the mean value.

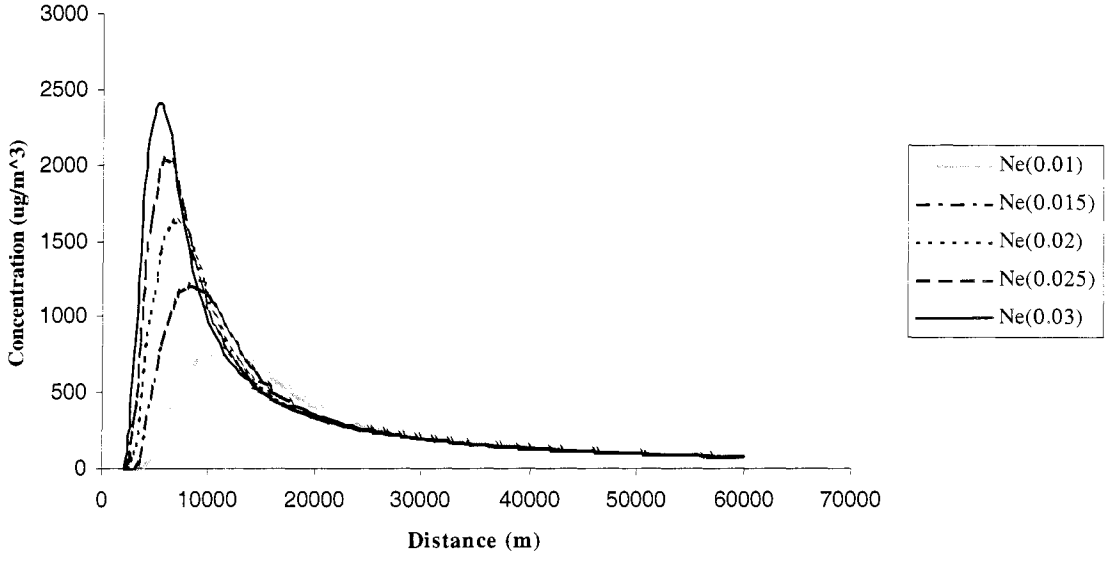

Figure 6.3 Model sensitivity to the parameter N_e (Sec^{-1})

6.2.4 Sensitivity Analysis of Parameter F_o :

The parameter of buoyancy flux depends on both the meteorological parameters such as ambient air density and the source parameters such as cross-sectional area of the stack and effluent density and velocity at stack exit.

The quantitative comparison, given in Table 6.4, shows that the lowest value of the buoyancy resulted into the highest ground level concentration and vice versa. A gradual shift in the maximum concentration location away from the stack from higher to lower buoyancy values is also seen from Table 6.4.

Table 6.4 Model Sensitivity to the parameter F_o: maximum concentrations and corresponding distances

F_o (m^4/Sec^3)	% Difference from the mean value	C_{max} ($\mu g/m^3$)	X_{max} (m)	% Difference of C_{max} from the concentration corresponding to mean value	%Difference of X_{max} from the distance corresponding to mean value
250.000	-50.00	2431.00	5500.00	48.96	-21.43
375.000	-25.00	1931.00	6000.00	18.32	-14.29
500.000	0.00	1632.00	7000.00	0.00	0.00
625.000	25.00	1422.00	7500.00	-12.87	7.14
750.000	50.00	1264.00	8000.00	-22.55	14.29

Note: (-) sign shows the decrease from the mean value.

Higher concentrations associated with lower buoyancy values may stem from the small plume rise and reduced dispersion of a plume in the stable layer. On the other hand, higher buoyancy will help in the plume rise and will increase the dispersion of the plume within the stable boundary layer resulting into the lower ground level concentrations at large distances.

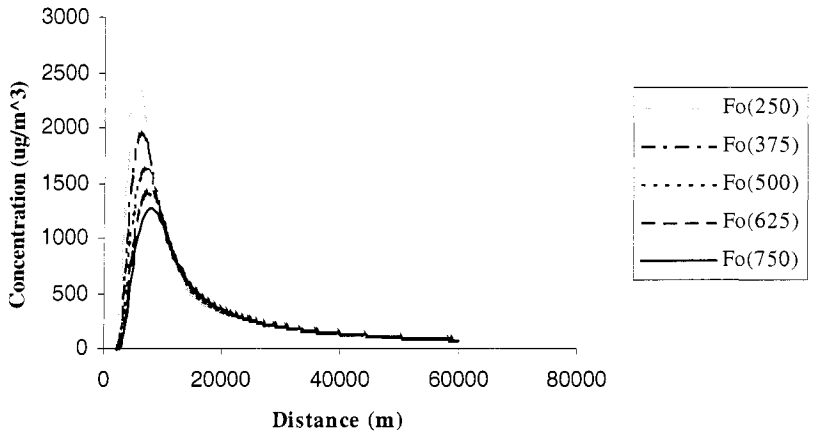

Figure 6.4 Model sensitivity to the parameter F_o ($m^4 Sec^{-3}$)

6.2.5 Sensitivity Analysis Of Parameter Q:

The use of emission rate (Q) allows explicitly drawing conclusion about the concentration magnitude since it is directly proportional to the concentration magnitude in the model expression. However changes in emission rates do not displace the maximum concentration location (c.f. Table 6.5). Model sensitivity to this parameter is shown in Figure 6.5.

Table 6.5 Model Sensitivity to the parameter Q: maximum concentrations and corresponding distances

Q (Kg/Sec)	% Difference from the mean value	C_{max} (ug/m^3)	X_{max} (m)	% Difference of C_{max} from the concentration corresponding to mean value	%Difference of X_{max} from the distance corresponding to mean value
1.750	-50.00	816.00	7000.00	-50.00	0.00
2.625	-25.00	1224.00	7000.00	-25.00	0.00
3.500	0.00	1632.00	7000.00	0.00	0.00
4.375	25.00	2040.00	7000.00	25.00	0.00
5.250	50.00	2448.00	7000.00	50.00	0.00

Note: (-) sign shows the decrease from the mean value.

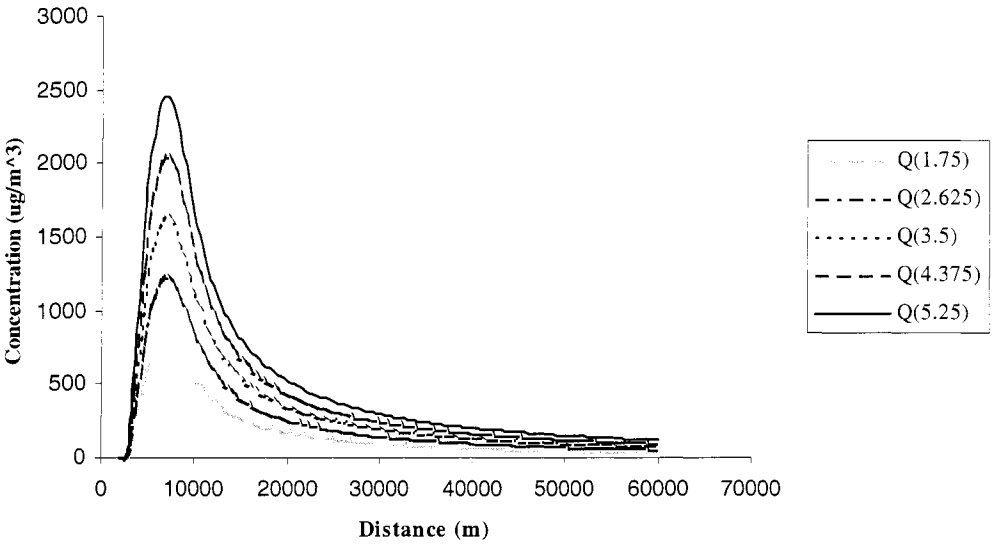

Figure 6.5 Model sensitivity to the parameter Q (Kg/Sec)

6.3 Discussion On Sensitivity Analysis Results:

Comparing all the results of sensitivity analysis in Table 6.6 and 6.7, the A_o variable used in the TIBL calculation appears to be the most sensitive variable based on the spatial displacement location of maximum concentration. Table 6.6 shows that by decreasing A_o value from 4 to 2 (i.e. 50 % decrease) C_{max} decreases by maximum from the C_{max} corresponding to the mean A_o approximately 50.6% (i.e. from 1632 $\mu g/m^3$ to 807 $\mu g/m^3$). Moreover, by decreasing A_o by 50% (i.e. from 4 to 2) the horizontal distance X_{max} corresponding to maximum concentration increases from 7000 m to 22000 m (i.e. ~214 % increase).

Similarly for the variables $\frac{U}{w_*}$, N_e and F_o, the 50% decrease in their magnitudes from the mean values result into maximum decrease of concentration (C_{max}) by ~15%, ~53.5% and maximum increase of ~ 49%, respectively, (c.f. Table 6.6). The 50% decrease in magnitudes result into maximum decrease of horizontal distances (X_{max}) by ~21.4% and ~21.4% for the variables of $\frac{U}{w_*}$ and F_o, respectively, and maximum increase of ~ 57% for the variable of N_e (c.f. Table 6.7). Magnitude of the maximum concentration is also sensitive to the parameter of emission rate (Q). The maximum concentration increases or decreases by the same percentage as the Q increases or decreases in the magnitude from the mean value. This shows that model results are proportional to Q. However, the change in emission rate has no impact on its location. The above stated facts are also shown in Figures 6.6 and 6.7.

Table 6.6 % Differences of maximum concentrations (C_{max}) from the mean values of the parameters in sensitivity analysis

% Difference from the mean value of the parameter	% Difference of C_{max} from the concentration corresponding to mean value				
	U/w_*	A_o	N_e	F_o	Q
-50	-14.83	-50.55	-53.49	48.96	-50
-25	-5.64	-22.67	-26.16	18.32	-25
0	0	0	0	0	0
25	3.19	13.36	24.88	-12.87	25
50	4.72	17.83	47.43	-22.55	50

Note: (-) sign shows the decrease from the mean value.

Table 6.7 % Differences of maximum horizontal distances (X_{max}) from the mean values of the parameters in sensitivity analysis

% Difference from the mean value of the parameter	%Difference of X_{max} from the distance corresponding to mean value				
	U/w^*	A_o	N_e	F_o	Q
-50	-21.43	214.29	57.14	-21.43	0
-25	-14.29	50	21.43	-14.29	0
0	0	0	0	0	0
25	7.14	-28.57	-14.29	7.14	0
50	14.29	-42.86	-21.43	14.29	0

Note: (-) sign shows the decrease from the mean value.

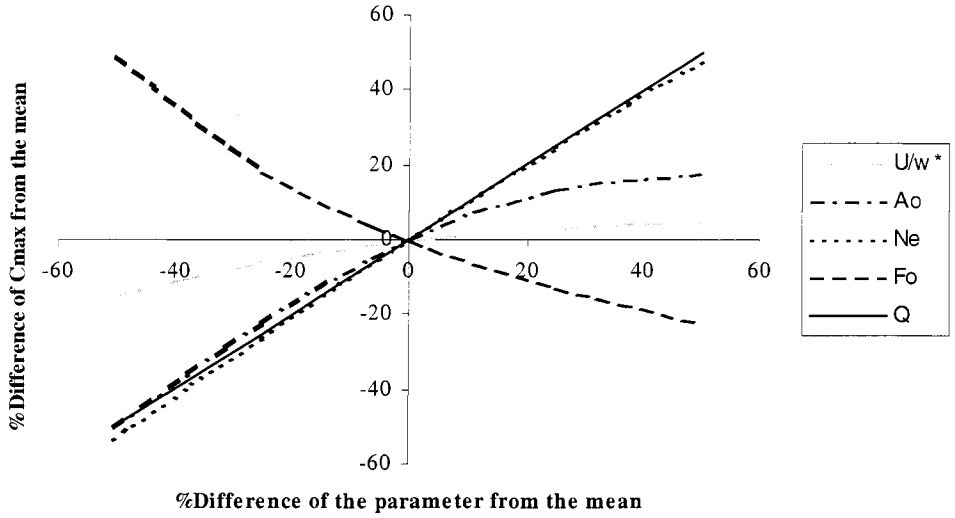

Figure 6.6 Plot of % Differences of maximum concentrations (C_{max}) from the mean values of the parameters in sensitivity analysis

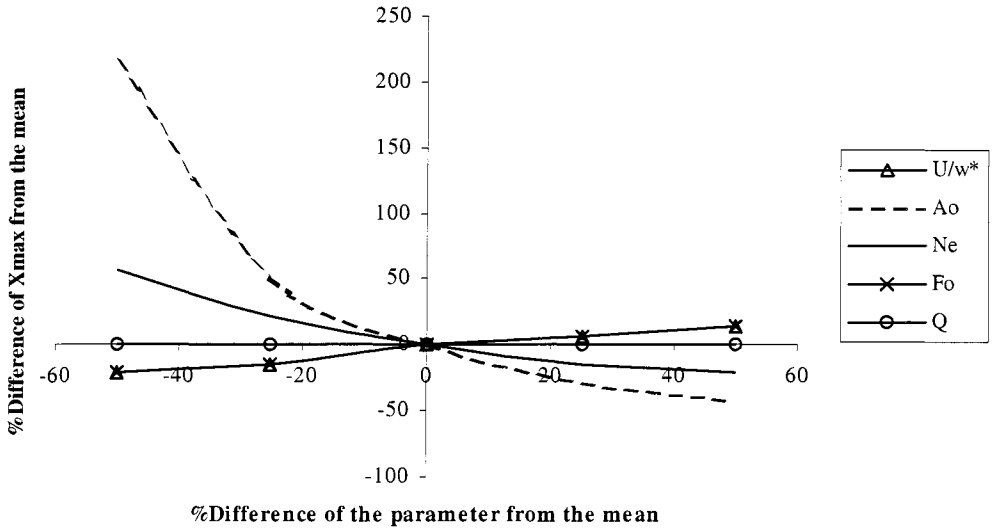

Figure 6.7 Plot of % Differences of maximum horizontal distances (X_{max}) from the mean values of the parameters in sensitivity analysis

Chapter 7

Fumig: A Software Tool for Fumigation Study

7.1 Introduction:

This chapter provides a general overview of the features of a computer software tool, named as Fumig, to predict the ground level concentration during the fumigation. This software is built upon the revised fumigation model discussed in Chapter 4. The code for Fumig is written and compiled in visual basic. It can be used for simulation and regulatory purposes within the coastal region.

7.2 The Basic Formulation of the Model:

The primary step in the fumigation modeling is to characterize the TIBL and this can be properly done through an estimate of the surface sensible heat flux (H). Unfortunately sensible heat flux cannot be measured directly. It depends on the net radiation (R_n). To calculate sensible heat flux, the formulation proposed by Oke (1978) and being used in AERMOD is adopted here.

$$H_f = \frac{0.9R_n}{(1+1/B_o)} \tag{7.1}$$

Where

B_o is Bowen Ratio

R_n is net radiation (W/m^2)

H_f is sensible heat flux (W/m^2)

The net radiation R_n is calculated by following the method of Holtslag and Van ulden (1983).

$$R_n = \frac{[1-r\{\phi\}]R_s + C_1 T_{ref}^6 - \sigma_{SB} T_{ref}^4 + C_2 n}{(1+C_3)} \tag{7.2}$$

Where

$C_1 = 5.31\times10^{-13} Wm^{-2}K^{-6}$

$C_2 = 60 Wm^{-2}$

$C_3 = 0.12$

$\sigma_{SB} = 5.67\times10^{-8} Wm^{-2}K^{-4}$ (Stefan Boltzman Constant)

T_{ref} = Ambient Air Temperature at ground surface (K)

$r\{\phi\}$ = Albedo

R_s = Solar Radiation

$n = (0.0-1.0)$ (Cloud Cover)

Solar radiation (R_s) corrected for cloud cover is taken from Kasten and Czeplak (1980).

$$R_s = R_o(1-0.75n^{3.4}) \tag{7.3}$$

$$R_o = 990 Sin\phi - 30 \tag{7.4}$$

Where

ϕ is solar elevation angle and $\phi = \frac{\phi[t_p]+\phi[t]}{2}$, $[t_p]$= previous hour and $[t]$=present hour.

Local solar elevation angle is determined from the principles of geometry and is given by Zahang and Anthes (1982) as:

$$\mathrm{Sin}\phi = \mathrm{Sin}\Psi\mathrm{Sin}\delta - \mathrm{Cos}\Psi\mathrm{Cos}\delta\mathrm{Cos}\left[\left(\frac{\pi t_{UTC}}{12}\right) - \lambda\right] \tag{7.5}$$

Where Ψ and λ are the latitude (positive north) and longitude (positive west) in radians, δ is the solar declination angle (angle of the sun above the equator, in radians), and t_{UTC} is coordinated universal time in hours.

The solar declination angle is given as:

$$\delta = \phi_r \mathrm{Cos}\left[\frac{2\pi(d - d_r)}{d_y}\right] \tag{7.6}$$

Where ϕ_r is the latitude of the Tropic of Cancer (23.45^o=0.409 radians), d is the number of the day of the year, d_r is the day of the summer solstice (173), and d_y is the average number of days per year (365.25).

The other characteristics of the model such as TIBL growth with distance inland; plume rise and concentration modeling, already discussed in chapter 4, are also incorporated in Fumig.

7.3 Fumig: Input Data Requirement:

The input data requirement is divided in four categories: 1) Meteorological data, 2) Source data, 3) Time information and 4) Grid location. Fumig input data sheet is shown in Figure 7.1.

7.3.1 Meteorological Data:

The following input parameters are required in meteorological section.

Bowen Ratio: The user is allowed to enter the value from 0.1 to 5. Typical values range from 5 over semi-arid regions, 0.5 over grasslands and forests, 0.2 over irrigated grass, and 0.1 over the sea.

Albedo: The model accepts a value in the range from 0.05 to 0.5. Its value varies from 0.4 over light-colored dry soils, 0.2 over grass and many agriculture crops, 0.1 over coniferous forests, to 0.05 over dark wet soils.

Surface Temperature: The lower bound on this parameter is 280 K and the upper bound is 323 K. Usually temperature ranges between these values in the summer during the daytime in the Northwestern hemisphere.

Wind Speed: The stability index $\frac{U}{w_*}$ (i.e. ratio between wind speed and convective velocity) should be greater than 1.2 to avoid stream-wise diffusion and less than 6 to fulfill the condition of strong convection for the applicability of the fumigation model. During vigorous heating at the ground, convective velocity can be on the order of 1 to 2 m/s. If the average value of convective velocity is considered as 1.5 m/s then the lower bound on the input wind speed value is 2 m/s and the upper bound is 8 m/s.

Potential Temperature Gradient: The model deals with the stable stratified over water flows so the range considered for this parameter is from 0.003 to 0.04 k/m.

Over Water Temperature: The minimum input value allowed is 273 k and the maximum value must be less than the surface temperature.

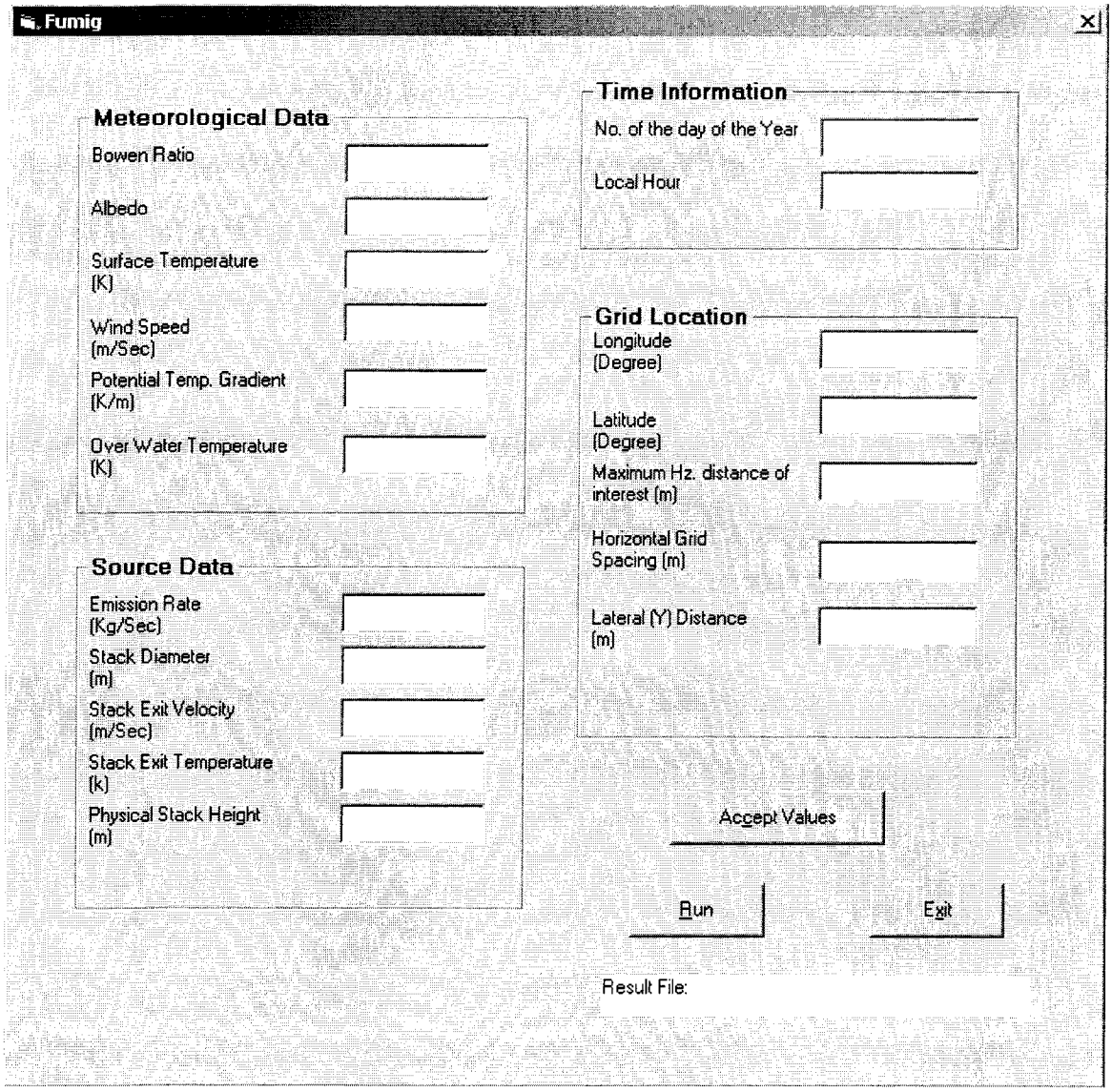

Figure 7.1 Input Data Sheet

7.3.2 Source Data:

The following input parameters are required under this category.

Emission Rate: The model accepts the source emission rate greater than 0 and equal or less than 20 kg/s.

Stack Diameter: Its value is expected between 1 to 15 m.

Stack Exit Velocity: It should be greater than 1.5 times of wind speed to avoid stack downwash.

Stack Exit Temperature: The gas exiting from the stack must be having temperature greater than the ambient over water air. The maximum value, which the model accepts is 1000K.

Physical Stack Height: The model considers elevated gas release from medium to tall stacks located on a shoreline. The Physical Stack height is limited to 30 m as minimum input value and 300 m as maximum value.

7.3.3 Time Information:

These input parameters are used in calculating the Surface heat flux.

Number of the Day of the Year: The fumigation model deals with summer season (June 22nd to September 21st). So the number of the day of the year must be greater than 173 (Julian day), which is considered as the day of summer solstice. The maximum value is 264, which corresponds to the 21st day of September.

Local Hour: This parameter measures the solar elevation angle. Its value ranges from 10 to 17. Sun is considered well above the horizon during this range.

7.3.4 Grid Location:

Longitude: The minimum acceptable value is 0 degree and maximum is 180 degree west. The negative sign is used for meridians on the west of the prime meridian as a usual sign convention. But the equation 7.5 considers the value of the longitude as a positive west to calculate the solar elevation angle.

Latitude: The value ranges from 0 to 90 degree north.

Maximum Horizontal Distance of Interest: This represents the maximum distance of interest along the mean wind direction. Its value must be greater than the distance of the fumigation zone. If a smaller value is entered then while computing the parameters a message of increasing the distance of interest will be appeared. The upper bound is 100000 m (~100Km).

Horizontal Grid Spacing: Its value is at least 10 (m). The maximum value should be less than the maximum horizontal distance of interest.

Lateral Distance: Its value is 0 if the user is interested in calculating the ground level concentrations along the plume centerline and this is the minimum input value for this parameter. The maximum value is 3000 (m).

7.4 Model Output:

Once the values are keyed into the program then the user has to click or press on the Accept Values button shown in Figure 7.2. If the input value is missing or a value of the parameter is out of the above-specified range, then a message box will be appeared on pressing the Accept Values button. The message box will prompt the user to enter the correct value for the parameter.

On the other hand if all the values are in the specified ranges then on clicking the Accept values button a message box will appear prompting the user to click Run button. After pressing on the Run button a file with the name of **Fumig.doc** will be opened and stored in the C root directory. The path and the name of the file will appear in the Result File box as shown in Figure 7.2.

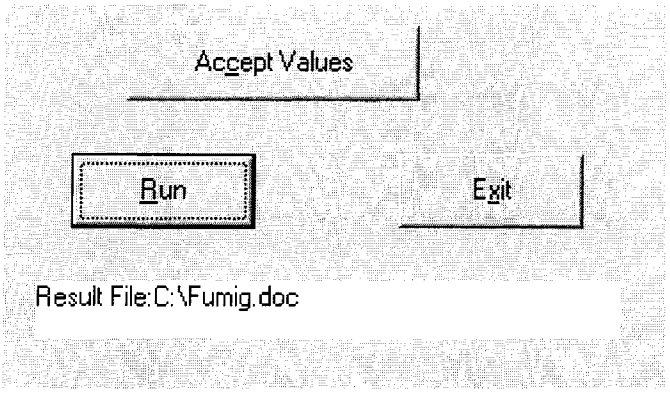

Figure 7.2 Enlarged view of control buttons and result file box of Fumig

Typical output of a Fumig run is presented in Appendix 6. The output file contains five categories of results.

The first category in the output file gives the values of meteorological parameters such as heat flux, Brunt Vaisala Frequency and Convective velocity.

The second category gives information about the fumigation zone. It includes the distance from the stack where fumigation starts and ends, the height at which the plume centerline intercepts the TIBL, and plume vertical dispersion coefficient and the horizontal distance from the stack corresponding to that height.

The third kind of the information in the output file is about the magnitude of the buoyancy flux.

The fourth section displays the magnitude of TIBL parameter (A_o), the equilibrium height of TIBL and the corresponding horizontal distance from the stack, and a table for TIBL height with distance inland.

The fifth and final section of the file gives ground level concentrations in ($\mu g/m^3$) along the horizontal distances from the stack at the specified lateral distance.

Chapter 8

Conclusions and Recommendations for Future Studies

8.1 Concluding Remarks:

The newly developed fumigation PDF model in the present study is based on approach that includes state-of-the art knowledge of TIBL turbulence and dispersion (analogous to CBL) in a simple framework. It is very time efficient and just requires a short time (few seconds) for computational purposes. It has been demonstrated that assumption of Weil and Brower's convective limit works fair-to-good for TIBL in the case of fumigation. The proposed model considers the condition of stable onshore flow and uses the Garratt's (1992) model to determine the height of TIBL. The model is best in predicting contaminant dispersion in stable onshore flows and strong convective conditions. The model also assumes that transport by bulk motion due to mean wind in the x direction, which is considered to be along the mean direction of wind, exceeds stream wise effective diffusion. Characterizing in terms of stability index of $\frac{U}{w_*}$, the model is applicable in the wide range of stability $1.2<\frac{U}{w_*}<6$.

The inclusion of vertical finite time scale T_{lz}, reduces the vertical dispersion and moves the point of maximum concentration downwind. A key assumption is $T_{lz}=T_{ly}$. As initially, vertical dispersion is reduced so at the large downwind distances more pollutant

is available to disperse. Due to this fact, higher concentrations at the large distances for finite Lagrangian time scale are observed than infinite Lagrangian time scale.

During the performance analysis of the model, normality test of residuals confirmed their normal distribution without any transformation. Residuals also showed nice scatter without funnel shape when plotted against predicted values of the model. Further, the analysis provided the evidence that they were independent of the input variables.

Both the mean absolute error and mean relative error are used as quantitative measures of coastal dispersion model performance, besides mean and standard deviation of Residuals. The error analysis proves that model is having minimum error relative to the observed values.

Sensitivity analysis shows that the TIBL height parameter (A_o) is the most sensitive parameter to the model output in terms of the change in location of maximum concentration. It is also highly sensitive to the magnitude of maximum concentration. The parameter A_o is calculated from wind speed (U), Sensible heat flux (H) and over water potential temperature gradient (γ). So these parameters should be measured or calculated with better precision. Both the parameters Brunt Viasala frequency (N_e) and emission rate (Q) are also sensitive to model output in terms of the maximum concentration magnitude. The variation in the magnitude of concentration is directly proportional to the variation in Q, but the location of maximum concentration does not vary.

For easy and effective use of the newly developed model, user-friendly computer software 'Fumig' is also developed. This software is coded in visual basic.

8.2 Recommendations:

1. Model should be extended to account for the fumigation phenomenon under near neutral onshore flow conditions.
2. Further development efforts should focus on incorporating the complex terrain treatment in the model, as model is limited to get concentration profiles over flat terrain.
3. The model ability should be extended to deal with plume rise from both the multiple sources and the stack with scrubber.

References

1. Baerentsen, J. H., and Berkowicz, R. (1984). Monte Carlo Simulation of Plume Dispersion in the Convective Boundary Layer. *Atmospheric Environment*, **18**,701-12.
2. Briggs, G.A. (1984). Plume Rise and Buoyancy Effects, in D. Randerson (ed.), Atmospheric Science and Power Production. US Dept. Of Energy, NTIS-DE84005177, 327-66.
3. Caughey, S. J., Kitchen, M., and Leighton, J., R. (1983). Turbulence Structure in Convective Boundary Layers and Implications for Diffusion. *Boundary Layer Meteorology*, **25**, 345-52.
4. Deardorff, J.W. (1974). Three Dimensional Numerical Study of the Height and Mean Structure of a heated Planetary Boundary Layer. *Boundary Layer Meteorology*, **7**, 81-106.
5. Deardorff, J.W., and Willis, G.E. (1975). A Parameterization of Diffusion into the Mixed Layer. *Journal of Applied Meteorology*, **14**, 1451-58.
6. Deardorff, J.W., and Willis, G.E. (1982). Ground level concentrations due to fumigation into an entraining mixing layer. *Atmospheric Environment*, **16**,1159-70.
7. Deardorff, J. W., and Willis, G.E. (1985). Further results from a laboratory model of the convective planetary boundary layer. *Boundary Layer Meteorology*, **32**, 205-36.
8. DiCristofaro, D.C., and Hanna, S. R. (1990). The Offshore and Coastal Dispersion (OCD) Model: Revisions and Evaluations. In Air Pollution and Its Application VIII, Van Dop, and D.G. Steyn, Eds., Plenum Press, New York, 759-68.
9. Draxler, R.R. (1976). Determination of Atmospheric Diffusion Parameters. *Atmospheric Environment*, **10**, 99-105.

10. Draper , R.N., and Smith , H. (1981). Applied regression analysis. 2nd Ed., John Wiely, NY.

11. Du, S., Wilson, J.D., and Yee, E. (1994). Probability Density Functions for Velocity in the CBL, and Implied Trajectory Models. *Atmospheric Environment*, **28**,1211-17.

12. Fisher, A. L., Parsons, M. C., Roberts, S. E., Shea. P. J., Khan. F. I., and Husain, T. (2003). 'Long-Term SO_2 Dispersion Modeling Over a Coastal Region', *Environmental Technology,* **24,** 1-11.

13. Garratt, J.R. (1992). The Atmospheric Boundary Layer. Cambridge university press, Cambridge,186-89.

14. Hibberd, M.F., and Luhar, A.K. (1996). A Laboratory Study and Improved PDF Model of Fumigation into a Growing Convective Boundary Layer. *Atmospheric Environment*, **30**,3633-49.

15. Hicks, B.B. (1985). Behavior of Turbulent Statistics in the CBL. *J. Climate & Applied Meteorology* , **24,** 607-14.

16. Holtslag, A.A.M., and Van ulden, A.P. (1983). A Simple Scheme for Daytime Estimates for the Surface Fluxes from Routine Weather Data. *Journal of Climate & Applied Meteorology*, **22**, 517-529.

17. Kerman, B.R. (1982). A Similarity Model of Shoreline Fumigation. *Atmospheric Environment*, **16**, 467-77.

18. Lamb, R.G. (1982). Diffusion in the Convective Boundary Layer. Atmospheric Turbulence and Air Pollution Modelling ,Nieuwstadat, F.T.M, and Van, D.H. (Eds.), D. Reidel Publishing Co, Dordrecht, The Netherlands, 159-29.

19. Li, K. Z., and Briggs. A. G. (1988). Simple Pdf Models for Convective Driven Vertical Diffusion. *Atmospheric Environment*, **22**,55-74.

20. Luhar, A.K., and Britter, R.E. (1990). An application of Lagrangian Stochastic Modeling to Dispersion during Shoreline Fumigation. *Atmospheric Environment*, **24A**, 871-81.

21. Luhar, A.K., and Sawford.B.L. (1995). Lagrangian Stochastic Modeling of the Coastal Fumigation Phenomenon. *J. of Applied Meteorology*, **34**,2259-2277.

22. Luhar, A.K., and Sawford, B.L. (1996). An Examination of Existing Shoreline Fumigation Models and Formulation of an Improved Model. *Atmospheric Environment*, **30**,609-20.

23. Luhar, A.K. (1998). An Analytical Slab Model For the Growth of the Coastal Thermal Internal Boundary Layer Under Near-Neutral Onshore Flow Conditions. *Boundary-Layer Meteorology*, **88**, 103-20.

24. Luhar, A.K. (2002). The Influence of Vertical Wind Direction Shear on Dispersion in The Convective Boundary Layer, and Its Incorporation in Coastal Fumigation Models. *Boundary-Layer Meteorology*, **102**, 1-38.

25. Luhar. A.K., and Young, S. A. (2002). Dispersion Moments of Fumigating Plumes-LIDAR Estimates And PDF Model Simulations. *Boundary-Layer Meteorology*, **104**, 411-44.

26. Lyons,W.A., and Cole, H. S. (1973). Fumigation and Plume Trapping on the shores of Lake Michigan during stable onshore flow. *J. of Applied Meteorology*, **12**,494-10.

27. Mason, P. J. (1992). Large Eddy Simulation of Dispersion in Convective Boundary Layers with Wind Shear. *Atmospheric Environment*, **26A**, 1561-71.

28. Misra, P.K. (1980). Dispersion from Tall Stacks into a Shoreline Environment. *Atmospheric Environment*, **14**, 397-00.

29. Misra, P.K. and Onlock, S. (1982). Modelling Continuous Fumigation of Nanticoke Generating Station Plume. *Atmospheric Environment*, **16**, 479-89.

30. Oke, T.R. (1978). Boundary Layer Climates, John Wiley and Sons, New York, 372.

31. Portelli, R. V. (1982). The Nanticoke Shoreline Diffusion Experiment, June, 1978-I: Experimental Design and Program Overview. *Atmospheric Environment*, **16**,413-21.

32. Stull, R.B. (1988). An Introduction to Boundary Layer Meteorology. Kluwer Academic Publishers, Dordrecht, The Netherlands, 450.

33. Taylor, G.I. (1921). Diffusion by Continuous Movements. *Proc. London Math Society, Ser. 2*, **20**, 196-12.

34. Venkatram, A.K. (1982). A Frame Work for Evaluating Air quality Models. *Boundary-Layer Meteorology*, **24**, 371-85.

35. Venkatram, A. (1977). A Model of Internal Boundary Layer Development, *Boundary Layer Meteorology*, **11**, 419–37.

36. Venkatram, A. (1988). Topics in Applied Dispersion Modeling. Lectures on Air Pollution Modelling A.Venkatram and J.C. Wyngaard, Eds., American Metrological Society, Boston, MA, 267-24.

37. Van, D. H., Steenkist, R., and Nieustadt E.T.M. (1979). Revised Estimates for Continuous Shoreline Fumigation. *J. of Applied Meteorology*, **18**,133-37.

38. Weil, J.C., and Brower, P.R. (1984). Estimating Convective Boundary Layer Parameters for Diffusion Applications. Maryland Power Plant Siting Program Rep. PPSP-MP-48, Dept. of Natural Resources, Annapolis, MD, 37.

39. Weil, J.C., and Corio, A. L. (1985). Dispersion Formulations Based on Convective Scaling. Maryland Power Plant Siting Program Rep. PPSP-MP-60, Dept. of Natural Resources, Annapolis, MD, 39.

40. Weil, J.C. (1988). Dispersion in the Convective Boundary Layer. Lectures on Air Pollution Modelling, A.Venkatram and J.C. Wyngaard, Eds., American Meteorological Society, Boston, MA, 167-27.

41. Weil, J.C. (1990). A Diagnosis of the Asymmetry in top-down and bottom-up diffusion using a Lagrangian Stochastic Model. *J. Atmospheric Science*, **47**,501-15.

42. Weil, J. C., Corio, L. A., and Brower, P. R. (1997). A PDF Despersion Model for Boyant Plumes in the Convective Boundary Layer. *J. of Applied Meteorology*, **36**, 982-1003.

43. Wyngaard, J.C. (1988). Structure of the PBL. Lectures on Air Pollution Modelling , A.Venkatram and J.C. Wyngaard, Eds., American Meteorological Society, Boston, MA, 9-61.

44. Zhang, D., and Anthes, R., A. (1982). A High-Resolution Model of the Planetary Boundary Layer-Sensitivity Tests and Comparisons with SESAME-79 Data. *Journal of Applied Meteorology*, **21**, 1594-1609.

Appendix 1

Expression for Entrainment Rate

Air density within the TIBL can be assumed constant analogous to ML within CBL. This allows the use of volume conservation in place of mass conservation. In a column of TIBL air of height, z_i, over a given horizontal area on the earth, A, the volume is $A*z_i$. If η is considered as the net volumetric flow rate into the volume, then volume conservation yields:

$$\eta = A\frac{dz_i}{dt} \tag{A-1.1}$$

Inflow occurs in the vertical because of entrainment at the top of the TIBL, and in the horizontal because of convergence within the TIBL. So in the absence of cloud cover:

$$\eta = w_e A - \int_{z=0}^{z_i} \iint_A \nabla_{xy} dx dy dz \tag{A-1.2}$$

Where ∇_{xy} is the divergence in horizontal plane and w_e is the rate at which the air entrained into the top of TIBL as discussed in section 1.4.2.

Continuity equation for the case of incompressible fluid flow states that horizontal divergence must be compensated by vertical shrinking or vertical convergence (subsidence). Mathematically:

$$\frac{\partial u}{\partial x} + \frac{\partial v}{\partial y} + \frac{\partial w}{\partial z} = 0 \tag{A-1.3}$$

Or

$$\frac{\partial u}{\partial x} + \frac{\partial v}{\partial y} = -\frac{\partial w}{\partial z} \tag{A-1.4}$$

From Equations (A-1.2) & (A-1.4):

$$\eta = w_e A - \int_{z=0}^{z_i} \iint_A -\frac{\partial w}{\partial z} dx dy dz \qquad \text{(A-1.5)}$$

Or

$$\eta = w_e A + \iint_A \int_{z=0}^{z_i} \frac{\partial w}{\partial z} dz dx dy \qquad \text{(A-1.6)}$$

Or

$$\eta = w_e A + w_z \iint_A dx dy \qquad \text{(A-1.7)}$$

Or

$$\eta = w_e A + w_z A \qquad \text{(A-1.8)}$$

Where w_z is the mean large vertical motion, acting on the top of TIBL (i.e., subsidence). Moreover the magnitude of w_z is negative for subsidence.

Upon combining Equations (A-1.1) and (A-1.8) and dividing by A, the following expression is obtained:

$$\frac{dz_i}{dt} = w_e + w_z \qquad \text{(A-1.9)}$$

When there is no subsidence or horizontal divergence is zero then Equation (A-1.9) can be written as:

$$\frac{dz_i}{dt} = w_e \qquad \text{(A-1.10)}$$

Equation (A-1.10) shows that the TIBL top rises at a rate equal to w_e in the absence of subsidence.

Equation (A-1.10) can be written into gradient equation as follows:

$$U\frac{dz_i}{dx} = w_e \tag{A-1.11}$$

Where U is the mean wind within the TIBL.

Expression for $z_i(x)$ from Equation (4.2) is given as:

$$z_i(x) = A_o x^{\frac{1}{2}} \tag{A-1.12}$$

Or

$$x^{\frac{1}{2}} = \frac{z_i(x)}{A_o} \tag{A-1.13}$$

From Equations (A-1.11) and (A-1.12)

$$w_e = U\frac{d(A_o x^{\frac{1}{2}})}{dx} \tag{A-1.14}$$

Or

$$w_e = \frac{1}{2}\frac{UA_o}{x^{\frac{1}{2}}} \tag{A-1.15}$$

Putting the expression for $x^{\frac{1}{2}}$ from Equation (A-1.13) into Equation (A-1.15), the entrainment rate is given as:

$$w_e = \frac{1}{2}\frac{UA_o^2}{z_i}$$

Appendix 2

Statistical Theory

A Lateral Dispersion:

Taylor's theory applies to the displacements of passive particles serially emitted from a point source in a turbulent flow. Further more, turbulence is considered homogeneous and stationary. As the turbulence is stationary so the autocorrelation coefficient of turbulent velocity of a fluid particle is a function of time lag. This defines the correlation between the particle velocity at one time v(t) and at some later time v(t+τ). Here τ is a time separation. For the y direction autocorrelation (R_v) is given by:

$$R_v = \frac{\langle v(t)v(t+\tau)\rangle}{\langle v^2\rangle} \qquad \text{(A-2.1)}$$

Where the angle brackets denote an ensemble mean. The ensemble average $\langle v(t) + v(t+\tau)\rangle$ means the average over a large number of trials of the product of the velocity of a single particle at t multiplied by the velocity of the same particle at time $t+\tau$. As the turbulence is considered homogeneous and stationary so both the mean ensemble average and time average would be the same.

As $\tau \rightarrow 0$, $R_v \rightarrow 1$ since the velocity is perfectly correlated with itself at zero lag, and as τ gets large, R_v approaches zero because the velocity becomes independent of its earlier value at time t. A measure of the time over which v becomes independent of its value at t is the Lagrangian integral time scale and may be given as:

$$T_{ly} = \int_0^\infty R_v(\tau)d\tau \qquad \text{(A-2.2)}$$

Since the particles are passive, they do not affect the flow and thus move with the local fluid velocity. Hence, the displacement y of the particle in one realization is:

$$y = \int_0^t v(T)dT$$

Mean ensemble average $\langle y \rangle$ is given by:

$$\langle y \rangle = \int_0^t \langle v(T) \rangle dT \qquad \text{(A-2.3)}$$

As $\langle v \rangle = 0$, so from Equation (A-2.3) the magnitude of $\langle y \rangle$ will also be 0.

Of course, at time t not all particles are in the same plane, nor will they be at the same distance from the source. Despite the average y coordinate is equal to zero for a large number of particles after a travel time t, no single particle arrives precisely at the mean position of the ensemble $(\bar{x},0)$ and aim is to quantify the lateral spread. The mean square displacement, which is the average of the square of a displacement due to turbulent velocity component, provides a tool to measure this spread. The mean square displacement in the y direction is the variance by definition:

$$\sigma_y^2 = \langle y^2 \rangle \qquad \text{(A-2.4)}$$

Even though the turbulence is stationary σ_y^2 will increase with time and is thus said to be evolutionary quantity.

Differentiating Equation (A-2.4) with respect to t gives:

$$\frac{\sigma_y^2}{dt} = 2\langle y \rangle \frac{d\langle y \rangle}{dt} \qquad \text{(A-2.5)}$$

Where $\frac{d\langle y\rangle}{dt} = \langle v(t)\rangle$ (A-2.6)

Or

$$\frac{\sigma_y^2}{dt} = 2\langle v(t)y(t)\rangle \quad \text{(A-2.7)}$$

Or

$$\frac{\sigma_y^2}{dt} = 2\int_0^t \langle v(t)v(t+\tau)\rangle d\tau \quad \text{(A-2.8)}$$

From Equation (A-2.1) the above expression can be written as:

$$\frac{\sigma_y^2}{dt} = 2\langle v^2\rangle \int_0^t R_v(\tau)d\tau \quad \text{(A-2.9)}$$

As stationary and homogeneous flow is considered so $\langle v^2\rangle$ is constant in the above equation.

Hence another integral yields:

$$\sigma_y^2 = 2\langle v^2\rangle \int_0^t \int_0^t R_v(\tau)d\tau dt \quad \text{(A-2.10)}$$

As the average of the square of the fluctuating component is its variance σ_v^2, so Equation (A-2.10) can be written as:

$$\sigma_y^2 = 2\sigma_v^2 \int_0^t \int_0^t R_v(\tau)d\tau dt \quad \text{(A-2.11)}$$

Two limiting forms of Equation (A-2.11) arise as the result of the $R_v(\tau)$ behaviour. For very small $T << T_{ly}$, $R_v \sim 1$ and Equation (A-2.11) yields:

$$\sigma_y^2 = 2\sigma_v^2 \int_0^t \int_0^t d\tau dt \quad \text{(A-2.12)}$$

Or

$$\sigma_y^2 = 2\sigma_v^2 \int_0^t t\,dt \qquad \text{(A-2.13)}$$

Or

$$\sigma_y^2 = \sigma_v^2 t^2 \qquad \text{(A-2.14)}$$

The root-mean-square lateral displacement (σ_y) due to the root–mean-square lateral velocity (σ_v) is given by:

$$\sigma_y = \sigma_v t \qquad \text{(A-2.15)}$$

Equation (A-2.15) states that the plume growth is linear with time.

For long (infinite) times, R_v approaches zero, but its integral remains finite and is given by Equation (A-2.2). Equation (A-2.11) reduces to:

$$\sigma_y^2 = 2\sigma_v^2 T_{ly} \int_0^t dt \qquad \text{(A-2.16)}$$

Where $T_{ly} = \int_0^{t\to\infty} R_v(\tau)d\tau$ is the lateral Lagrangian Integral time scale.

Or

$$\sigma_y^2 = 2\sigma_v^2 T_{ly} t \qquad \text{(A-2.17)}$$

$$\sigma_y = \sqrt{2T_{ly}}\,\sigma_v t^{\frac{1}{2}} \qquad \text{(A-2.18)}$$

So in this time limit, σ_y grows parabolically with t, which is a diffusive type of behavior.

A convenient function f_{ly} is used (Weil, 1988) to account for both the short and long term ranges. So, The root-mean-square lateral displacement ($\sigma_y = \langle y^2 \rangle^{\frac{1}{2}}$) due to the root–mean-square lateral velocity ($\sigma_v = \langle v^2 \rangle^{\frac{1}{2}}$) is given by:

$$\sigma_y = \sigma_v \frac{t}{f_{ly}} \qquad \text{(A-2.19)}$$

B Vertical Dispersion:

The above stated Lagrangin concept for the particle trajectory in the vertical direction is applied here for the dispersion in the convective boundary layer.

The root-mean-square vertical displacement (σ_z) due to the root–mean-square vertical turbulent velocity (σ_w), at small time scale (when $R_w \rightarrow 1$ similar to R_v), is given by:

$$\sigma_{zj} = \sigma_{wj} t \qquad \text{(A-2.20)}$$

Where j=1,2 is representing updraft and downdraft respectively.

In the previous fumigation models the Equation (A-2.20) was assumed to hold true even at long times and the key assumption was the infinite vertical Lagrangian time scale.

Using the earlier explanation, Equation (A-2.18) may be used for the root-mean-square displacement in the vertical direction for the finite time scale as:

$$\sigma_{zj} = \sqrt{2T_{lz}}\,\sigma_{wj} t^{\frac{1}{2}} \qquad \text{(A-2.21)}$$

The function f_{lz} similar to the function f_{ly}, which accounts for both the short and long time ranges, is used here.

$$\sigma_{zj} = \sigma_{wj} \frac{t}{f_{lz}} \tag{A-2.22}$$

C Solution of a Differential Equation Governing a Particle Trajectory in the Vertical Direction Considering Finite T_{lz} :

Consider the following equation governing the particle trajectory.

$$\int_{z_s}^{z} dz = \int_{0}^{t} w(t)dt \tag{A-2.23}$$

In the case of infinite vertical Lagrangian time scale it is assumed that at any time downwind $R_w \rightarrow 1$. This implies that the vertical velocity at any time downwind is perfectly correlated with its value at the source height and independent of time. So, the Equation (A-2.23) may be rewritten as:

$$\int_{z_s}^{z} dz = w\int_{0}^{t} dt \tag{A-2.24}$$

Or

$$z - z_s = wt \tag{A-2.25}$$

Conversely, in the vertical finite Lagrangian time scale, $R_w \rightarrow 1$ only at short times and approaches to zero at large times. So, at large times vertical velocity cannot be correlated with its value at the source height and obviously becomes time dependent. Even though $R_w \rightarrow 0$ at large times but its integral remains finite and is given as:

$$T_{lz} = \int_{0}^{t\rightarrow\infty} R_w(\tau)d\tau \tag{A-2.26}$$

Where T_{lz} is the vertical Lagrangian Integral time scale.

To deal with both the short and long times the T_{lz} effect should be included in the solution of Equation (A-2.23). A convenient function f_{lz} (which has already been used in the statistical theory) is introduced here in the solution of Equation (A-2.23). This simple function accounts the statistics of T_{lz} in stationary and homogenous turbulent flows. The solution of Equation (A-2.23) may be presented as:

$$z - z_s = \frac{wt}{f_{lz}} \tag{A-2.27}$$

It's important to note that, in stationary and homogeneous turbulence the statistical properties depend only on the displacements in time and space and not on the initial time or position.

Appendix 3

Expression for the Elemental Source Strength (dQ)

From Equation (4.7) the elemental source strength at the plume-TIBL interface is mathematically given as:

$$dQ(x',y',z') = \left(K_{zs}\frac{\partial C_s}{\partial z} + U_s C_s \frac{dz_i(x')}{dx} \right)\Delta x'\Delta y'$$

$$dQ(x',y',z') = C_s\left(\frac{K_{zs}}{C_s}\frac{\partial C_s}{\partial z} + U_s \frac{dz_i(x')}{dx} \right)\Delta x'\Delta y' \qquad \text{(A-3.1)}$$

The solution of the term $\left(\frac{K_{zs}}{C_s}\frac{\partial C_s}{\partial z} \right)$ in Equation (A-3.1) is given as follows;

$$K_{zs} = \frac{1}{2}\frac{d\sigma_{zf}^2}{dt} \qquad \text{(A-3.2)}$$

Assuming a constant mean wind speed in the stable layer, Equation (A-3.2) is written as:

$$K_{zs} = \frac{1}{2}U_s\frac{d\sigma_{zf}^2}{dx'} \qquad \text{(A-3.3)}$$

Or

$$K_{zs} = U_s\sigma_{zf}\frac{d\sigma_{zf}}{dx'} \qquad \text{(A-3.4)}$$

A Gaussian model gives concentration profile within the stable layer, so expression for C_s:

$$C_s(x',y',z;H) = \frac{Q}{2\pi U_s \sigma_{yf}\sigma_{zf}}\exp\left[-\frac{(z-H)^2}{2\sigma_{zf}^2} - \frac{y'^2}{2\sigma_{yf}^2} \right] \qquad \text{(A-3.5)}$$

In writing the Equation (A-3.5) it is assumed that material entrained into the TIBL cannot affect the concentration in the stable layer, so there is no reflection term is included.

$$\frac{\partial C_s}{\partial z} = \frac{Q}{2\pi U_s \sigma_{yf} \sigma_{zf}} \exp\left[-\frac{(z-H)^2}{2\sigma_{zf}^2} - \frac{y'^2}{2\sigma_{yf}^2} \right] \frac{\partial}{\partial z}\left[-\frac{(z-H)^2}{2\sigma_{zf}^2} - \frac{y'^2}{2\sigma_{yf}^2} \right] \tag{A-3.6}$$

Or

$$\frac{\partial C_s}{\partial z} = \frac{Q}{2\pi U_s \sigma_{yf} \sigma_{zf}} \exp\left[-\frac{(z-H)^2}{2\sigma_{zf}^2} - \frac{y'^2}{2\sigma_{yf}^2} \right]\left[-\frac{(z-H)}{\sigma_{zf}^2} \right] \tag{A-3.7}$$

From Equations (A-3.4) and (A-3.7) the term $\left(\frac{K_{zs}}{C_s} \frac{\partial C_s}{\partial z} \right)$ becomes:

$$\frac{K_{zs}}{C_s} \frac{\partial C_s}{\partial z} = U_s \sigma_{zf} \frac{d\sigma_{zf}}{dx'}\left[-\frac{(z-H)}{\sigma_{zf}^2} \right] \tag{A-3.8}$$

Or

$$\frac{K_{zs}}{C_s} \frac{\partial C_s}{\partial z} = U_s \frac{d\sigma_{zf}}{dx'}\left[-\frac{(z-H)}{\sigma_{zf}} \right] \tag{A-3.9}$$

Putting back this expression into Equation (A-3.1);

$$dQ = C_s\left[U_s \frac{d\sigma_{zf}}{dx'}\left[-\frac{(z-H)}{\sigma_{zf}} \right] + U_s \frac{dz_i(x')}{dx'} \right] \Delta x' \Delta y' \tag{A-3.10}$$

As here the interest is in calculating the concentration at plume-TIBL interface so z will be replaced by $z_i(x')$.

$$dQ = C_s U_s\left[\frac{dz_i(x')}{dx'} - \frac{d\sigma_{zf}}{dx'} \frac{(z_i(x') - H(x'))}{\sigma_{zf}} \right] \Delta x' \Delta y' \tag{A-3.11}$$

Defining the term $\left[\frac{(z_i(x') - H(x'))}{\sigma_{zf}}\right]$ as $p(x')$ Equation (A-3.11) takes the form;

$$dQ = C_s U_s \left[\frac{dz_i(x')}{dx'} - \frac{d\sigma_{zf}}{dx'} p(x')\right] \Delta x' \Delta y' \tag{A-3.12}$$

Here $\frac{dQ}{\Delta x' \Delta y'}$ is defined as a Flux 'F (x',y')' associated with the elemental area $\Delta x' \Delta y'$.

$$F(x', y') = C_s U_s \left[\frac{dz_i(x')}{dx'} - \frac{d\sigma_{zf}}{dx'} p(x')\right] \tag{A-3.13}$$

Or

$$F(x', y') = C_s U_s \frac{1}{\sigma_{zf}} \left[\frac{dz_i(x')}{dx'} - \frac{d\sigma_{zf}}{dx'} p(x')\right] \sigma_{zf} \tag{A-3.14}$$

Now let's assume;

$$G(x') = \frac{1}{\sigma_{zf}} \left[\frac{dz_i(x')}{dx'} - \frac{d\sigma_{zf}}{dx'} p(x')\right] \tag{A-3.15}$$

Adding the term of $\frac{1}{\sigma_{zf}} \frac{dH(x')}{dx'}$ on both sides of Equation (A-3.15), $G(x')$ is given as;

$$G(x') = \frac{1}{\sigma_{zf}} \left[\frac{dz_i(x')}{dx'} - \frac{d\sigma_{zf}}{dx'} p(x')\right] + \frac{1}{\sigma_{zf}} \frac{dH(x')}{dx'} - \frac{1}{\sigma_{zf}} \frac{dH(x')}{dx'} \tag{A-3.16}$$

Or

$$G(x') = \frac{1}{\sigma_{zf}} \left[\frac{dz_i(x')}{dx'} - \frac{d\sigma_{zf}}{dx'} p(x') - \frac{dH(x')}{dx'}\right] + \frac{1}{\sigma_{zf}} \frac{dH(x')}{dx'} \tag{A-3.17}$$

Putting back the expression for $p(x')$ in Equation (A-3.17), $G(x')$ is given as;

$$G(x') = \frac{1}{\sigma_{zf}} \left[\frac{dz_i(x')}{dx'} - \frac{dH(x')}{dx'} - \frac{(zi(x') - H(x'))}{\sigma_{zf}} \frac{d\sigma_{zf}}{dx'}\right] + \frac{1}{\sigma_{zf}} \frac{dH(x')}{dx'} \tag{A-3.18}$$

Or

$$G(x') = \frac{\left[\sigma_{zf}\left[\frac{dz_i(x')}{dx'} - \frac{dH(x')}{dx'}\right] - \left[\frac{(zi(x') - H(x'))}{\sigma_{zf}}\frac{d\sigma_{zf}}{dx'}\right]\right]}{\sigma_{zf}} + \frac{1}{\sigma_{zf}}\frac{dH(x')}{dx'} \qquad \text{(A-3.19)}$$

Or

$$G(x') = \left[\frac{\sigma_{zf}\left[\frac{dz_i(x')}{dx'} - \frac{dH(x')}{dx'}\right] - \left[(z_i(x') - H(x'))\frac{d\sigma_{zf}}{dx'}\right]}{\sigma_{zf}^2(x')}\right] + \frac{1}{\sigma_{zf}}\frac{dH(x')}{dx'} \qquad \text{(A-3.20)}$$

The first term on the right hand side of Equation (A-3.20) is the derivative of the term $\left[\frac{(z_i(x') - H(x'))}{\sigma_{zf}(x')}\right]$ with respect to dx′

$$G(x') = \frac{d}{dx'}\left[\frac{(Zi(x') - H(x'))}{\sigma_{zf}(x')}\right] + \frac{1}{\sigma_{zf}}\frac{dH(x')}{dx'} \qquad \text{(A-3.21)}$$

Or

$$G(x') = \frac{dp(x')}{dx'} + \frac{1}{\sigma_{zf}}\frac{dH(x')}{dx'} \qquad \text{(A-3.22)}$$

If the plume attains the final rise before touching the lower portion of the TIBL then the second term on the right hand side of Equation (A-3.22) will be dropped out and the parameterization for term G(x′) would be the same as given by Misra (1980). Otherwise Misra's (1980) model incorrectly uses $G(x') = \frac{dp(x')}{dx'}$.

Appendix 4

Parameters Defining the w PDF

The four out of six unknown parameters in Equation (4.21) (i.e. λ_1, λ_1, $\overline{w_1}$ and $\overline{w_2}$) are found by equating the zeroth through third moment (i.e. $\overline{w^n} = \int_{-\infty}^{\infty} w^n p_w(w)dw$; n=0-3) of that bi-Gaussian distribution with the followings:

$$\overline{w^0} = \lambda_1 + \lambda_2 = 1 \tag{A-4.1}$$

$$\overline{w^1} = 0 \tag{A-4.2}$$

$$\overline{w^2} = \sigma_w^2 = 0.31 w_* \text{ (Under convective limit)} \tag{A-4.3}$$

$$\overline{w^3} = S\sigma_w^3 \tag{A-4.4}$$

The other two unknown parameters in Equation (4.21) (i.e. σ_{w1} and σ_{w2}) are parameterized by Weil (1990) as follows:

$$\sigma_{w1} = R\overline{w_1} \tag{A-4.5}$$

$$\sigma_{w2} = R\left|\overline{w_2}\right| \tag{A-4.6}$$

Weil (1990) solutions for the mean vertical velocities in updrafts $\overline{w_1}$ and downdrafts $\overline{w_2}$ are given by the following expressions, respectively:

$$\frac{\overline{w_1}}{\sigma_w} = \frac{\alpha_W S}{2} + \frac{1}{2}\left(\alpha_W^2 S^2 + \frac{4}{\beta_W}\right)^{\frac{1}{2}} \tag{A-4.7}$$

$$\frac{\overline{w_2}}{\sigma_w} = \frac{\alpha_W S}{2} - \frac{1}{2}\left(\alpha_W^2 S^2 + \frac{4}{\beta_W}\right)^{\frac{1}{2}} \tag{A-4.8}$$

Where

$$\alpha_W = \frac{1+R^2}{1+3R^2}\ ; \qquad \beta_W = 1+R^2$$

σ_w and S are averaged vertical velocity standard deviation and skewness, respectively.

The parameter R is defined as:

$$R = \frac{\sigma_{w1}}{\overline{w_1}} = \frac{\sigma_{w2}}{\left|\overline{w_2}\right|} \tag{A-4.9}$$

Subscripts 1 and 2 are associated with updrafts and downdrafts.

Weil et al. (1997) laboratory analysis shows good agreement between the modeled and measured crosswind integrated concentrations under strong convection at R=1.

Assuming R=1, the magnitude of α_W and β_W turnout to be 0.5 and 2 respectively. The magnitude of S is taken as 0.6 from the Minnesota experiments (Wyngaard, 1988). Under Weil and Brower's (1984) convective limit ($u_* \sim 0$), σ_w from Equation (4.22) is:

$$\sigma_w = 0.56 w_* \tag{A-4.10}$$

Putting back these values of α_W, β_W, S and σ_w in Equations (A-4.7) and (A-4.8), the following expressions are obtained:

$$\overline{w_1} = 0.488 w_* \tag{A-4.11}$$

$$\overline{w_2} = -0.32 w_* \tag{A-4.12}$$

Weighting coefficients for the updraft and downdraft distributions λ_1 and λ_2, respectively, are given as follows:

$$\lambda_1 = \frac{\overline{w_2}}{w_2 - w_1} \cong 0.4 \tag{A-4.13}$$

$$\lambda_2 = -\frac{\overline{w_1}}{w_2 - w_1} \cong 0.6 \qquad \text{(A-4.14)}$$

With R=1 Equations (A-4.5 and A-4.6) result out:

$$\sigma_{w1} = \overline{w_1} = 0.488 w_* \qquad \text{(A-4.15)}$$

$$\sigma_{w2} = \overline{|w_2|} = 0.32 w_* \qquad \text{(A-4.16)}$$

Appendix 5

Matlab Code

```
%inputs required by a user
q=input ('Enter the value of emission rate Kg/s\n');
A=input ('Enter the value of A\n');
u=input ('Enter the average wind speed (m/s) \n');
wasto=input ('Enter the value of W* (m/s) \n');
fo1=input ('Enter the bouyancy flux for the First stack \n');
fo2=input ('Enter the bouyancy flux for the Second stack \n');
omga=input ('Enter the Value of Brunt Vaisala Frequency \n');
sheight=input ('enter the value of source height(m)\n');
y=input ('enter the value of lateral distance(m)\n');
distint=input ('Distance of Interset (m)\n');
G_spa=input ('Horizontal Grid Spacing\n');
nostp=round(distint/G_spa);
z=0;
%calculation of TIBL height
tast=600; %convective scale time in sec.
zieq=wasto*tast;%equilibrium height of Tibl
xieq=(zieq/A)^2; %distance where equilibrium height is achieved
stpsize=distint/nostp;
  hcalc=zeros(1,nostp+1);
  distcalc=zeros(1,nostp+1);
  for i=1:length(hcalc);
    hcalc(i)=A*sqrt(stpsize*(i-1));
    distcalc(i)=stpsize*(i-1);
     end;
     hcalc;

%Calculation of final plume rise
%The Nanticoke power plant plume achieves final rise before intercepting its lower part with TIBL.
omgasq=omga^2;
fpr1=2.4*((fo1/(u*omgasq))^0.3333333); %final plume rise scheme from Misra (1982) for Stack 1
fpr2=2.4*((fo2/(u*omgasq))^0.3333333); %final plume rise from Misra (1982) for Stack 2
fpr=(fpr1+fpr2)/2;
zio=sheight+fpr; %height where plume center line intersects with TIBL top
xio=(zio/A)^2;    %distance corresponding to height zio
fo=(fo1+fo2)/2;
znprime=(1.3*(fo^(1/3))/u)*(xio^(2/3));
sigmazfo=0.5*fpr;          %vertical dispersion coefficient for stable layer from Misra (1982)
ratsigzfo=(sigmazfo/zio);
sigyfo=0.5*(1.3*(fo^(1/3))*(xio^(2/3))*(u^-1));        from Misra (1982)
ratsigyfo=(sigyfo/zio);
zinmin=(zio-1.4*sigmazfo); %TIBL height which corresponds to hz distance where fumigation starts
zinmax=(zio+1.4*sigmazfo); %TIBL height which corresponds to hz distance where fumigation ends
xinmin=(zinmin/A)^2 ;%horizontal distance where fumigation starts
xinmax=(zinmax/A)^2; %horizontal distance where fumigation zone ends.
We=(0.5*u*(A^2))/zio;
rato=We/wasto;
xdec=(xinmin>=distcalc);
if xdec(end)==1;
   disp('\n Plz re-run the program and Increase the Horizontal Distance of Interest');
```

```
else;
cp1=(xinmin<distcalc);
[mval1 ind1]=max(cp1);
cp2=(xinmax<distcalc);
[mval2 ind2]=max(cp2);
if (ind1==ind2);
   disp('you have not selected any point within the fumigation zone. Plz re-run the program and decrease
the spacing');
else;
cp3=(zieq<hcalc);
      [mval3 ind3]=max(cp3);
if (mval3==1);
  hcalc(1,ind3:end)=zieq;
end;
xfumig1=distcalc(ind1:(ind2-1));
xfumig=[xfumig1];
zfumig1=hcalc(ind1:(ind2-1));
zfumig=[zfumig1];
cp4 =(xinmax<distcalc);
[mval4 ind4]=max(cp4);
if (mval4==1);
        xtrap1=distcalc(ind4:end);
        ztrap1=hcalc(ind4:end);
end;
xtotal=[xfumig xtrap1];
ztotal=[zfumig ztrap1];
%writing to output file
fid = fopen('Fumig.rtf','wt'); % opening the output file
fprintf (fid,'Hz distance at TIBL equilibrium height= %10.3f(m)\n',xieq);
fprintf (fid,'TIBL equilibrium height= %10.3f(m)\n',zieq);
fprintf (fid,'\n Plume Rise at the intersection of TIBL= %10.3f(m)\n',fpr);
fprintf (fid,'\nValue of A= %10.3f(m)\n',A);
fprintf (fid,'\nZio= %10.3f(m)\n',zio);
fprintf (fid,'\nXio= %10.3f(m)\n',xio);
fprintf (fid,'\nVertical dispersion coefficient for stable layer @Zio=%10.3f(m)\n',sigmazfo);
fprintf (fid,'\nLateral dispersion coefficient for stable layer @Zio=%10.3f(m)\n',sigyfo);
fprintf (fid,'\n Non-dimensional vertical dispersion coefficient for stable layer
@Zio=%10.3f(m)\n',ratsigzfo);
fprintf (fid,'\n Non-dimensional lateral dispersion coefficient for stable layer
@Zio=%10.3f(m)\n',ratsigyfo);
fprintf (fid,'\nConvective vel @ Zio=%10.3f(m)\n',wasto);
fprintf (fid,'\nEntrainment vel=%10.3f(m)\n',We);
fprintf (fid,'\nRatio of entrainment vel to convective vel=%10.3f(m)\n',rato);
fprintf (fid,'\nDistance from the shoreline where fumigation zone starts= %10.3f(m)\n',xinmin);
fprintf (fid,'\nDistance from the shoreline where fumigation zone ends= %10.3f(m)\n',xinmax);
fprintf (fid,'\nTIBL height at the starting of fumigation zone= %10.3f(m)\n',zinmin);
fprintf (fid,'\nTIBL height at the ending of fumigation zone= %10.3f(m)\n',zinmax);
fprintf(fid,'\nTABLE OF TIBL HEIGHT WITH IN FUMIGATION ZONE\n\n');
cp5=(xinmax<=xtotal);
[mval5 ind5]=max(cp5);
cp6=(xinmax==xtotal);
cp7=[cp6 0];
[mval7 ind7]=max(cp7);
fprintf(fid,'\nDistance(m)  Concentration(ug/m^3)\n');
fprintf(fid,'========== ========================\n');
for ii=1:length(xtotal);
```

```
if (ii<ind5) | (mval5==0); % Concentration calculations within the Fumigation Zone
   xbtzon=xfumig;
   zbtzon=zfumig;
   xtrap=xbtzon(ii);
   ztrap=zbtzon(ii);
   stepfumig=(xtrap-xinmin)/50;
   xprimel=zeros(1,51);
   for kk=1:length(xprimel);
     zprimel(kk)=A*((xinmin+stepfumig*(kk-1))^0.5);
      xprimel(kk)=xinmin+stepfumig*(kk-1);
   end;

   xpri=xprimel(1:end-1);
   zpri=zprimel(1:end-1);
      [conc1] = pdfsf(u,sheight,wasto,y,z,fo,fpr,zpri,xpri,ztrap,xtrap);
   conc1;
   conc1a=[conc1 0];
      xpri1a=[xpri xprimel(end)];
   elseif ( cp7(ii)==1); % Concentration calculations out of the Fumigation Zone
     xbtzon=xfumig;
   zbtzon=zfumig;
   xtrap=xbtzon(ii);
   ztrap=zbtzon(ii);
   stepfumig=(xtrap-xinmin)/50;
   xprimel=zeros(1,51);
   for kk=1:length(xprimel);
     zprimel(kk)=A*((xinmin+stepfumig*(kk-1))^0.5);
      xprimel(kk)=xinmin+stepfumig*(kk-1);
   end;

   xpri=xprimel(1:end-1);
   zpri=zprimel(1:end-1);
      [conc1] = pdfsf(u,sheight,wasto,y,z,fo,fpr,zpri,xpri,ztrap,xtrap); % Calling the Function pdfsf
   conc1;
   conc1a=[conc1 0];
      xpri1a=[xpri xprimel(end)];
   else

   xtrap=xtotal(ii);
   ztrap=ztotal(ii);
   stepfumig=(xinmax-xinmin)/50;
   xprimel=zeros(1,51);
   for kk=1:length(xprimel);
     zprimel(kk)=A*((xinmin+stepfumig*(kk-1))^0.5);
      xprimel(kk)=xinmin+stepfumig*(kk-1);
   end;

   xpri=xprimel(1:end);
   zpri=zprimel(1:end);

         [conc1] = pdfsf(u,sheight,wasto,y,z,fo,fpr,zpri,xpri,ztrap,xtrap);

      conc1a=[conc1];
      xpri1a=[xpri];
   end;
```

```
anticonc1=trapz(xpri1a,conc1a);%integral of concentration values with respect to xprime.
conc2=(1/(2*pi))*anticonc1;%Concentration values after incorporating all the source pts
conc=conc2*q*(10^9);% concentration in micro gram per cubic meters.
fprintf (fid,'\n%10.2f %10.4f\n',xtrap,conc);

end;
end;
end;
fclose(fid);
```

Matlab Code for Function pdfsf

```
% Function pdfsf used in Fumig to compare the Nanticoke results.
function [conc1] = pdfsf(u,sheight,wasto,y,z,fo,fpr,zpri,xpri,ztrap,xtrap);
repit=[-4:4];
znprime=(1.3*(fo^(1/3))/u).*(xpri.^(2/3));

      znprime(1,1:end)=fpr;
      sigzfxp=0.5.*znprime;
                              hxp=sheight+znprime;
  %this section calculates the term s(x') in the pdf fumigation model of Luhar 2002.
  for     l=1:length(xpri);
          sxp(l)=(zpri(l)-hxp(l))/sigzfxp(l);
    sxpsq(l)=(sxp(l)^2);
    sols(l)=exp(-0.5*sxpsq(l));
  end
  %this section calculates the term G(x')in the pdf fumigation model.
  n=length(xpri);
  dsxp=diff(sxp)./diff(xpri); %derivative of term s(x') wrt x'
  adsxp=[dsxp(1) dsxp];
  dhxp=diff(hxp)./diff(xpri);%average value of derivative of plume rise H(x') wrt x'.
  adhxp=[dhxp(1) dhxp];%average value of derivativeof H(x') wrt x'
  for l=1:length(xpri);
          gxp(l)=adsxp(l)+((1/sigzfxp(l))*adhxp(l));
  end

  for jj=1:length(repit);
  for l=1:length(xpri);
    for m=1:length(xtrap) ;

  wast(m)=wasto;%convective velocity.
  w1avg(m)=0.488*wast(m);%mean vertical velocity in updrafts
  sigw1(m)=w1avg(m);%std. deviationin of vertical velocity comp. in updrafts
  w2avg(m)=-0.32*wast(m);%mean vertical velocity in downdrafts
  sigw2(m)=abs(w2avg(m));%std. deviationin of vertical velocity comp. in downdrafts


    %calculation of vertical velocity component in updraft(w1)
                  fyf1(l,m)=(wast(m)/ztrap(m))*((xtrap(m)-xpri(l))/u);
        fy(l,m)=(1+0.71*fyf1(l,m))^(1/2);
     w1(jj,l,m)=(z-zpri(l)+ 2*repit(jj)*ztrap(m))*((u/(xtrap(m)-xpri(l)))*fy(l,m));
  %calculation for shear dispersion coeff.
  %calculation for turbulent dispersion coeff.
  sigyt(l,m)=0.56*wast(m)*((xtrap(m)-xpri(l))/u)*(1/fy(l,m));
  sigytsq(l,m)=(sigyt(l,m))^2;
```

```
   sigyf(l)=0.5*(1.3*(fo^(1/3))*(xpri(l)^(2/3))*(u^-1));
   sigyfsq(l)=sigyf(l)^2; % calculation for lateral spread in the stable region
          sigpsq(l,m)=sigyfsq(l)+sigytsq(l,m);%term sigma '(x,x')
    sigp(l,m)=sigpsq(l,m)^0.5;
    a1=0.4; % fraction of area of updrafts
   fact1=a1/(sqrt(2*pi));
   a2=0.6;
   fact2=a2/(sqrt(2*pi));
                    w2(jj,l,m)=(-z-zpri(l)+ 2*repit(jj)*ztrap(m))*(u/(xtrap(m)-xpri(l)))*fy(l,m);
                      w1t1(jj,l,m)=(fact1/sigw1(m))*(exp(-((w1(jj,l,m)-
w1avg(m))^2)/(2*(sigw1(m)^2)))+exp(-((w2(jj,l,m)-w1avg(m))^2)/(2*(sigw1(m)^2))));
         w2t1(jj,l,m)=(fact2/sigw2(m))*(exp(-((w1(jj,l,m)-w2avg(m))^2)/(2*(sigw2(m)^2)))+        exp(-
((w2(jj,l,m)-w2avg(m))^2)/(2*(sigw2(m)^2))));
                        end
      end
   end
   totw=w1t1+w2t1;
   solw=sum (totw);
   for jj=1;
    for l=1:length(xpri);
      for m=1:length(xtrap);

     pw(jj,l,m)=solw(jj,l,m);%solution of pdf model for w

      end;
   end;
   end;
     for jj=1;
               for l=1:length(xpri);
           for m=1:length(xtrap);
        conc1(jj,l,m)=(gxp(l)*fy(l,m)/(xtrap(m)-xpri(l)))*(1/sigp(l,m))*sols(l)*exp(-
0.5*(y^2)/sigpsq(l,m))*pw(jj,l,m);
                        end;
               end;
      end;
```

Appendix 6

Typical Output Result File (Fumig.doc)

```
"1. METEOROLOGICAL PARAMETRS"

"Heat Flux (W/m^2)",188.208
"Brunt Vaisala Frequency (1/Sec)",.015
"Convective Velocity (m/Sec)",1.13
-------------------------------------------------------------------------
---

"2. INFORMATION ABOUT FUMIGATION ZONE"

"Fumigation Starts at a Distance (m)",2463.497
"Fumigation Ends at a Distance (m)",8984.052
"Plume Centerline intercepts the TIBL at Height (m) Zio",276.272
"Hz. Distance Xio (m) corresponding to Zio",5214.13
"Plume Veritcal Dispersion Coefficient at Zio",61.695
-------------------------------------------------------------------------
---

"3. STACK OUTPUT PARAMETER"

"Buoyancy Flux (m^4/Sec^3)",335.596
-------------------------------------------------------------------------
---

"4. TIBL OUTPUT PARAMETERS"

"TIBL height parameter A (m^0.5)",3.826
"Equilibrium height of TIBL(m)",677.459
"Hz. Distance Corresponding to equilibrium height of TIBL(m)",31352.601

"TABLE FOR TIBL HEIGHT"
Hz Distance(m)              TIBL Height(m)
===============             ===============
 0                           0
 1000                        120.989
 2000                        171.104
 3000                        209.559
 4000                        241.978
 5000                        270.54
 6000                        296.362
 7000                        320.107
 8000                        342.209
 9000                        362.967
 10000                       382.601
 11000                       401.276
 12000                       419.119
 13000                       436.233
```

14000	452.7
15000	468.589
16000	483.957
17000	498.851
18000	513.313
19000	527.379
20000	541.08
21000	554.442
22000	567.489
23000	580.243
24000	592.723
25000	604.946
26000	616.926
27000	628.678
28000	640.214
29000	651.546
30000	662.685
31000	673.639
32000	677.459
33000	677.459
34000	677.459
35000	677.459
36000	677.459
37000	677.459
38000	677.459
39000	677.459
40000	677.459
41000	677.459
42000	677.459
43000	677.459
44000	677.459
45000	677.459
46000	677.459
47000	677.459
48000	677.459
49000	677.459
50000	677.459
51000	677.459
52000	677.459
53000	677.459
54000	677.459
55000	677.459
56000	677.459
57000	677.459
58000	677.459
59000	677.459
60000	677.459
61000	677.459
62000	677.459
63000	677.459
64000	677.459
65000	677.459
66000	677.459
67000	677.459

68000	677.459
69000	677.459
70000	677.459
71000	677.459
72000	677.459
73000	677.459
74000	677.459
75000	677.459
76000	677.459
77000	677.459
78000	677.459
79000	677.459
80000	677.459
81000	677.459
82000	677.459
83000	677.459
84000	677.459
85000	677.459
86000	677.459
87000	677.459
88000	677.459
89000	677.459
90000	677.459
91000	677.459
92000	677.459
93000	677.459
94000	677.459
95000	677.459
96000	677.459
97000	677.459
98000	677.459
99000	677.459
100000	677.459

"5. CONCENTRATION PROFILE"

Latertal Distance (m): 0

Distance (m)	Concentration in Ug/m^3)
3000	0.1073
4000	255.2327
5000	966.8712
6000	1614.6564
7000	2063.9605
8000	2303.2161
9000	2363.1942
10000	2295.3719
11000	2133.293
12000	1899.5326
13000	1657.2195
14000	1444.7473

15000	1269.136
16000	1126.1666
17000	1009.5195
18000	913.4819
19000	833.4859
20000	766.0292
21000	708.4623
22000	658.7833
23000	615.4715
24000	577.362
25000	543.5537
26000	513.3412
27000	486.1665
28000	461.583
29000	439.2291
30000	418.8092
31000	400.0792
32000	388.4655
33000	380.6033
34000	373.2161
35000	366.2505
36000	359.663
37000	353.4169
38000	347.4813
39000	341.8297
40000	336.4392
41000	331.2896
42000	326.3632
43000	321.6441
44000	317.118
45000	312.7721
46000	308.5945
47000	304.5747
48000	300.7028
49000	296.97
50000	293.3678
51000	289.8887
52000	286.5258
53000	283.2724
54000	280.1225
55000	277.0705
56000	274.1113
57000	271.2399
58000	268.452
59000	265.7433
60000	263.1098
61000	260.5481
62000	258.0545
63000	255.626
64000	253.2596
65000	250.9525
66000	248.702
67000	246.5058
68000	244.3614

69000	242.2667
70000	240.2197
71000	238.2185
72000	236.2612
73000	234.3462
74000	232.4718
75000	230.6364
76000	228.8387
77000	227.0773
78000	225.3509
79000	223.6583
80000	221.9983
81000	220.3697
82000	218.7716
83000	217.203
84000	215.6628
85000	214.1502
86000	212.6644
87000	211.2045
88000	209.7696
89000	208.3592
90000	206.9723
91000	205.6085
92000	204.2669
93000	202.947
94000	201.6481
95000	200.3698
96000	199.1113
97000	197.8722
98000	196.6521
99000	195.4503
100000	194.2664